Process Optimization of Urea-Gradient SEC for Protein Refolding

Master Thesis

in Pharmaceutical Biotechnology

submitted by

Dominik Wilms

Hamburg-Bergedorf, Faculty of Life Sciences

February 28, 2012

Diese Arbeit wurde betreut und erstellt im Labor für Organische Chemie und Biochemie des Arbeitskreises für Aufarbeitungs- und Reinigungsverfahren an der Fakultät Life Sciences der Hochschule für Angewandte Wissenschaften (HAW) Hamburg.

1. Gutachter: Prof. Dr. rer. nat. Birger Anspach

2. Gutachter: Prof. Dr. phil. nat. Oliver Ullrich

Eidesstattliche Erklärung – *Declaration of Academic Honesty*

Hiermit erkläre ich an Eides statt, dass ich die vorliegende Arbeit eigenständig, ohne fremde Hilfe und ausschließlich unter Verwendung der angegebenen Hilfsmittel und Quellen angefertigt habe. Wörtlich oder dem Sinn gemäß aus anderen Werken entnommene Stellen sind unter Angabe der Quellen kenntlich gemacht.

Dominik Wilms

Hamburg, den 28. Februar 2012

Danksagung – *Acknowledgments*

Mit den nachfolgenden Zeilen darf ich mich bei einigen Menschen bedanken und damit ausdrücken, dass weder Studium noch Abschlussarbeit ohne fortwährende Unterstützung möglich sind.

Besonderer Dank gilt meinem Betreuer, Herrn Prof. Dr. Birger Anspach. Der Verlauf der Thesis erhielt zahlreiche Anregungen aus den fachlichen Diskussionen, aber auch persönlichen Gesprächen der vergangenen Monate. Viele positive Erfahrungen und nicht zuletzt auch *„Murphy's Law"* werde ich auch über das Studium hinaus mitnehmen.

Bei Herrn Prof. Dr. Oliver Ullrich möchte ich mich für das Übernehmen der Zweitkorrektur der Arbeit bedanken.

Weiterhin danke ich den Studenten und Mitarbeitern des OCB-Labors, deren Entgegenkommen und Hilfsbereitschaft den Alltag stets freundlich gestaltet haben.

Meiner Familie danke ich ganz herzlich für die kleinen und großen Gesten, die Vieles erleichtert haben. Ein besonderes Wort des Dankes gebührt dabei meinen Großeltern. Außerdem möchte ich mich bei meiner „kleinen" Schwester, Verena, für ihre Aufmerksamkeit und Freundschaft bedanken.

Täglichen Rückhalt gab und gibt mir der Optimismus, die Zuneigung und das Verständnis meiner Freundin, Sarah, der ich dafür von ganzem Herzen danke.

Table of Contents

List of Tables

List of Figures

List of Abbreviations

alpha-LA	-	α-lactalbumin
beta-LG	-	β-lactoglobulin
CCCD	-	central composite circumscribed design
CD	-	circular dichroism
CHAPS	-	3-[(3-cholamidopropyl)dimethylammonio]-1-propanesulfonate
CP	-	center point
CV	-	column volume
Dsb	-	disulfide bond
EDTA	-	ethylenediaminetetraacetic acid
ELISA	-	enzyme-linked immunosorbent assay
HEPES	-	4-(2-hydroxyethyl)-1-piperazineethanesulfonic acid
HEWL	-	hen egg-white lysozyme
GdnHCl	-	guanidinium hydrochloride
GSH	-	glutathione, reduced form (monomer)
GSSG	-	glutathione, oxidized form (dimer)
IB	-	inclusion body
PDB	-	Protein Data Bank
pI	-	isoelectric point
PMMA	-	Poly(methyl methacrylate)
SDS	-	sodium dodecyl sulfate
SEC	-	size-exclusion chromatography
TRIS	-	Tris(hydroxymethyl)aminomethane
UV/Vis	-	ultra-violet/visible light
V_0	-	interstitial or void volume of the SEC packed bed
V_m	-	total volume of the mobile phase in the SEC packed bed
λ_{max}	-	wavelength of maximum fluorescence intensity

1. Introduction

Much effort was taken within the last three decades in order to improve cell densities and product concentrations of bioprocesses aiming at higher mass yields of target proteins. Constantly enhanced techniques in cellular and molecular biology allowed for significant increases in target gene expression rates, while proceedings in process engineering evolved advances in peripheral issues. As these attempts became more and more successful (SHILOACH & FASS, 2005; CHOI et al., 2006) a critical observation came into focus of researchers and manufacturers: Heterologously produced proteins are frequently deposited in an aggregated, inactive form within the host cell as so called inclusion bodies. Consequently, renaturing proteins for the purpose of re-establishing its biological functionality became an increasingly important task for the industrial production of high-value proteins. Therefore, in recent years, a broad variety of different methods and procedures has been developed and applied to address the problem of regaining biological activity of target proteins.

The application of size-exclusion chromatography (SEC) as a refolding tool is generally assumed to be helpful due to its ability to physically separate folding intermediates within the pore system volume, thereby reducing aggregation effects and improving the overall renaturation success (GAO et al., 2003; CHEN & LEONG, 2010; year; FREYDELL et al., 2010). A previous work (WILMS, 2010) demonstrated a deviant result. When comparing SEC resins with various pore sizes, a desalting medium with a nominal pore size excluding all tested proteins gave best renaturation yields with the application of a urea-gradient SEC method for lysozyme refolding. The work presented in the following aimed at a procedural optimization of this technique as well as the subsequent transfer of the advanced method design to the refolding of further test proteins.

2. Theoretical Background

As being partly based on a preceding study of WILMS (2010), it has to be pointed out that some of the general information given in the following paragraphs of chapter 2 was mainly summarized from or has to be considered as an addition to the content of the reference cited above.

2.1 Formation of Inclusion Bodies

One of the most widely used host organisms for recombinant DNA technology is *Escherichia coli*. Since the 1970s, extensive experiences with its cultivation and genetic manipulation yielded steadily improved experimental protocols. The resulting ease of handling and the well-studied genome of *E. coli* nowadays enable researchers and manufacturers to establish efficient recombinant production processes with high cell densities and target protein concentrations. However, the required and achieved boost of expression rates frequently overloads natural folding pathways, thereby leading to the formation of dense insoluble particles, the so called inclusion bodies (IBs) (JUNGBAUER & KAAR, 2007; VASQUEZ et al., 2011).

It is generally assumed that IBs are aggregates of polypeptide chains which are misfolded completely or in parts. Unfolded or incorrectly folded strains combine with folding intermediates in partially native-like states so that the arising aggregate mainly consists of an oligomeric complex of a broad range of target protein conformations. Furthermore, it was suggested that IB formation bears strong resemblance to seeded polymerization in which small initial aggregates serve as nuclei for further accretion of non-native monomers (SPEED et al., 1996). Due to this sort of chain reaction, usually very few copies of IBs are present per cell (see figure 2-1). In living cells most likely only one or two aggregation sites are formed in the cyto- and/or periplasm, whereby spherical and stretched shapes are predominant, respectively. The size of an IB is commonly in the range of 0.1 to

1.5 µm and is dependent on various factors, i.e. expression rates, cell type and environmental conditions. There is evidence for intact native-like secondary structures and even binding sites within some IBs, whereas others do not show any patterned characteristics. Regardless of the either amorphous or amyloid-like structure, the aggregates tend to be insoluble in aqueous environment and devoid of biological activity (KOPITO, 2000; SINGH & PANDA, 2005).

For protein production purposes the latter implies the necessity of further efforts to regain the physiological functionality. Although this inevitably reduces the overall target protein yield, as any additional purification step does, today large scale protein synthesis with the deliberate appearance of IBs is a common practice in industry and research. Obviously this is primarily owed to some major advantages that can possibly come along with IB formation. First of all, separation of the target protein from host cell debris and proteins is relatively simple due to density differences. Moreover, deposition in aggregated form allows target protein shares of 30-50 % of total cell protein because the dense particulate form provides protection from protease degradation and the inactivity prevents the host from cytotoxic effects (MISAWA & KUMAGAI, 1999; LI et al., 2004; SINGH & PANDA, 2005). After mechanical disintegration of host cells, for example by sonification, French press or high pressure homogenizator for small, medium or large scale, respectively, IBs can be separated from cell debris at high degree of purification. Commonly slow speed centrifugation, filtration or chromatography techniques are applied for this separation step (RINAS & BAILEY, 1992; LI et al., 2004). Under appropriate conditions target protein purity after the first capture from host cells can be as high as 90 %. The remaining portion is owed to the fact that IBs do not purely consist of target protein

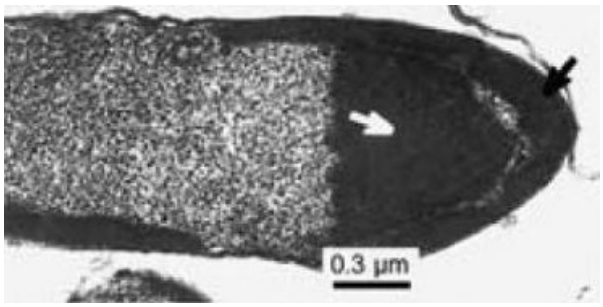

Fig. 2-1: Cytoplasmic (white arrow) and periplasmic (black arrow) inclusion bodies of Penicillin G acylase in *E. coli* cells. (modified from SRIUMOLBAS et al., 1997)

but include traces of other proteins and incorporated hydration water, soluble salts and amino acids (MISAWA & KUMAGAI, 1999).

In terms of economic management, for each production task a decision is to be made between avoiding the deposition of target protein into IBs *a priori* and establishing a protocol sequence for refolding into native-like or at least bioactive conformation. The former frequently suffers from unsatisfying product yields, while the latter might improve final product yields drastically but may be cumbersome and elaborate.

2.2 Solubilization of Inclusion Bodies

Assuming that renaturation of target protein from IBs is the method of choice, the first objective is turning the aggregated polypeptide chains into a water soluble state. This actually allows the application of liquid handling procedures which is on the one hand a major requirement for a reproducible and automatable process design and on the other hand provides the basis for the separation of aggregated components into a monomeric, refoldable form.

The most common method to achieve the goal of resolubilizing aggregated proteins is the treatment with strong chaotropic reagents. So called denaturants like guanidinium hydrochloride (GdnHCl) or urea in concentrations of 6 or 8 M, respectively, cause an effective disturbance of the highly organized water molecules surrounding the accessible IB surface. The strongest non-covalent protein and aggregation stabilizing effect, the internal hydrophobic interaction, is decreased (MIDDELBERG, 2002; TIMASHEFF & XIE, 2003; WANG & CHENG, 2010).

Subsequently, the polypeptide chains unfold but might still remain attached to each other due to intact non-native intermolecular disulfide bonds (Dsb). This is true for IBs of most periplasmic *E. coli* host proteins as well as recombinant proteins (LILIE et al., 1998). For a complete separation into polypeptide monomers the simultaneous treatment with a reducing agent is mandatory for such proteins

containing reactive cysteine residues in their amino acid sequence. Routinely, the addition of low molecular weight thiol reagents, most commonly dithiothreitol (DTT) or β-mercaptoethanol, is used to dissolve all disulfide bonds and keep cysteine residues in their reduced form (CABRITA & BOTTOMLEY, 2004).

The undefined conformational states of a resolubilized target protein in denatured and reduced monomeric form are usually termed random coils (TSUMOTO et al., 2002). Chemical unfolding as described above affects higher order structure of proteins only without splitting any peptide bonds. Other denaturation promoting effects can be applied, too, like shifting pH and/or temperature. Heat-induced increase in chain flexibility as well as changes in surface charge or conformation through pH variation can improve accessibility for and thereby effectiveness of denaturation reagents. However, attention must be paid thoroughly to not irreversibly destroy the protein's amino acid sequence by hydrolysis or thermal denaturation. As one consequence, the choice of an adequate buffer solution for both, de- and renaturation, is – besides economic considerations – essentially determined by the buffered pH range, which has to be in compliance with target protein requirements. In general, HEPES, TRIS or phosphate based buffers are prevailing (VALLEJO & RINAS, 2004; SINGH & PANDA, 2005).

According to Anfinsen's findings the remaining intact polypeptide primary structure contains all information necessary to autonomously fold back to its thermodynamically most stable conformation, i.e. its native state (ANFINSEN, 1973; ANFINSEN and SCHERAGA, 1975). This assumption generally describes denaturation as a reversible process. Nevertheless, in the very most cases accurately defined, protein-specific conditions must be provided to allow correct refolding.

2.3 Renaturation to Active Conformation

As being stated above, denaturation including disulfide reduction is reversible under precise modulation of various parameters. Consequently, successful *in vitro* refolding of proteins is dependent on the frequently elaborate task of providing specific renaturation-promoting conditions and a well-adapted experimental setup with a highly reproducible process sequence at best. The difficulty to cope with is the conversion of resolubilized but still inactive target protein into soluble products folded correctly to a native or at least bioactive conformation. Complications most frequently occur when the chaotropic denaturant is removed. Contemporary folding theories suggest that protein folding takes place along an energetic model termed free-energy funnel (see figure 2-2).

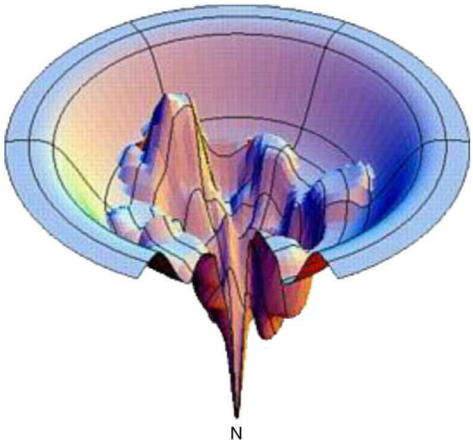

Fig. 2-2: Example of a so called free-energy funnel. Denatured protein states possess high energy, here represented by the funnel's upper rim. Through folding, the thermodynamic energy state of the protein molecule decreases and the protein virtually migrates down the funnel – potentially confronted with kinetic traps, which can result in aggregation-prone folding intermediates instead of native (N) conformation. (taken from CHAN & DILL, 1998)

Along this landscape of folding intermediates the native protein structure is expected to form at lower free energy states (CHAN & DILL, 1998; DOBSON, 2004). Yet, while folding back from the unfolded state, a protein can become kinetically trapped in an aggregation-prone intermediate conformation – especially when facing environmental conditions, which do not appear during the natural folding pathway. The competing folding and (re-)aggregation reactions are shown in figure 2-3.

In general, any refolding procedure aims at the best possible avoidance of the formation of intermediates predisposed for aggregation, thereby minimizing the loss of renatured protein yield. A thermodynamic status has to be established, shifting the

reaction equilibrium towards the favored development of the native protein conformation (QORONFLEH et al., 2007).

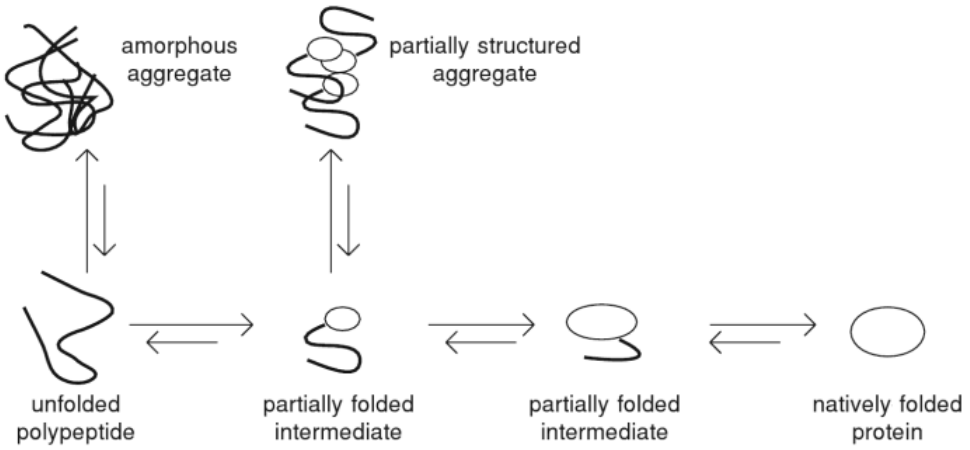

Fig. 2-3: Scheme illustrating the interrelation of the kinetic pathways between the native protein conformation and aggregate formation into differently structured morphologies. In addition, sometimes even highly structured fibrils are observable upon misfolding from intermediate states. Arrows indicate typically observed equilibrium tendencies. However, reversibility is a multi-parametric issue. (modified from MURPHY & TSAI, 2006)

Aiming at this goal in practice, the denaturation step is followed by the controlled removal of chaotropic denaturants in the presence of so called folding additives. However, low concentrations (1-2 M) of urea or GdnHCl are frequently upheld in refolding buffers with respect to their proven ability to inhibit aggregate formation. The concentration range within which residual chaotropes may act beneficial to the protein refolding success might be narrow. Thus, elaborate adjustment to refolding candidates is typically required (DE BERNARDEZ CLARK, 2001; SINGH & PANDA, 2005).
In case of target proteins containing natural or genetically engineered disulfide bonds, the exchange of the reducing agent DTT against a redox system facilitating disulfide bond reformation is an important factor determining renaturation yields. Most favored is a so called oxido-shuffling system, a mixture of reduced and oxidized glutathione, which is a pseudo tripeptide, found in almost all living cells. Its reduced monomeric form (GSH) consists of glutamic acid, cysteine and glycine and forms covalent dimers (GSSG) via bonding of cysteines under oxidizing conditions.

Establishing an environmental compartment, which contributes to disulfide formation, is glutathione's primary role in natural folding pathways. Three- to ten-fold excess of GSH over GSSG are typical ratios for *in vitro* folding approaches (CABRITA & BOTTOMLEY, 2004, BULAJ, 2005; QORONFLEH et al., 2007). Additionally, working at a slightly alkaline pH is favorable for the (re)formation of disulfide bonds due to the increased nucleophilic reactivity of thiol groups under these conditions (VALLEJO & RINAS, 2004; WANG et al., 2006; WANG et al., 2009). The amount of time needed for complete oxidative re-establishment of disulfide bonds is another factor with considerable impact on refolding experiments as it affects the total process duration as well as the suitable moment for performing analysis measurements. Recently, DING et al. (2008 and 2011) proposed a delay of about 20 hours between the end of an experiment and sample analysis for the refolding of lysozyme. Finally, the required folding progress and the associated kinetic time-frame, within which interaction with a shuffling system is particularly important for the reformation of native disulfide bonds, are generally unknown (BULAJ, 2005).

Additional folding-promoting reagents mentioned before may include certain low molecular weight substances known to inhibit intermolecular interactions responsible for protein aggregation. Some amino acids, especially L-arginine, presumably suppress aggregation by shielding hydrophobic regions of folding intermediates (DE BERNADEZ CLARK et al., 1999). Others, like proline, and chemical amino acid derivates, like glycine betaine, ecoin or firoin can serve as so called compatible solutes, which are solubility-improving osmolytes not directly interfering with proteins. Beyond these, some chelating agents (i.e. EDTA) or detergents, including CHAPS, SDS or Triton X-100, are other popular examples of numerous additives used in renaturation experiments. Besides these generally applicable folding aids, some target proteins might need very specific supplementary additives for proper folding, e.g. ions or cofactors stabilizing intermediate or final conformations. Any additive, whether a cosolute, preservative, surfactant or specific ligand, interferes with and modulates the protein structure and protein-protein

interactions, and thus has an effect on the refolding success. However, to what extent a refolding-promoting agent is beneficial for a particular renaturation objective has to be elucidated empirically, as they are not equally advantageous for all proteins. The interaction mechanisms of these additives with the folding intermediates remain often unclear, although their effectiveness has been proven in individual cases (ARAKAWA & TSUMOTO, 2003; SU et al., 2011)

Generally, the usage of these additives suffers from the increased costs and complexity of purification in order to remove them from final storage solutions. The same is true for an even more expensive variant of folding helpers: Molecular chaperones, either natural (e.g. GroEL, GroES or derivates) or artificial (e.g. cyclodextrin), facilitate proper folding through ATP-mediated cycles of binding and release of intermediate states, thereby suppressing aggregation reactions without actually changing folding pathways (THOMAS et al., 1997; SAMUEL et al., 2000; DONG et al., 2002).

Unwanted aggregation side reactions kinetically compete with proper folding and are therefore usually the main limitation to efficient renaturation. Though, since experimental as well as environmental conditions have substantial impact on the extent of misfolding and aggregate formation, various refolding parameters can be optimized in order to shift equilibrium towards correct, native-like folding (THOMAS et al., 1997). Low protein concentrations generally increase renaturation yields, because second or higher order kinetics of aggregation reactions dominate over first order folding at high concentrations. A major drawback to working at low concentrations is the subsequent reduction in the final concentration of successfully refolded protein. Quantitative specifications defining low and high concentrations are, of course, highly dependent on the target protein and its characteristics. In addition to the low concentration approach, working at low temperatures can improve refolding yields by the resulting reduction of hydrophobic interactions. However, prolonged overall time consumption has to be taken into account, especially for industrial applications. Moreover, exact composition and pH

adjustment of the denaturation and refolding buffers may affect target protein recovery. Some rather unusual procedures even make use of high pressure up to 4000 bar to facilitate the reestablishment of a native-like conformation by reducing steric hindrance effects physically (MALAVASI et al.; 2011). Finally, it is the choice of method(s), which influences the renaturation success (QORONFLEH et al., 2007; JUNGBAUER & KAAR, 2007).

At present days, a wide range of techniques favoring the correct refolding pathway is known and applied in manifold versions. Ease of handling and the lack of comparably successful alternatives made dilution methods the most commonly used renaturation approaches in industry and research for several decades. Currently, pulse-fed techniques came into focus, allowing relatively high final protein concentrations via dilution procedures (CHEN & LEONG, 2010). In addition to dilution of denatured and reduced protein samples in refolding-promoting buffer preparations, also dialysis against those buffers is often applied for laboratory scale refolding (LI et al., 2004). However, chromatographic procedures have some major advantages, though they can be elaborate for setup and optimization: Being easily automatable and scalable to different size while enabling minimization of buffer consumption are important characteristics of economically oriented processes and furthermore preferable for those manufacturing steps subject to (authority) validation. Moreover, in some cases adsorption chromatography as well as size-based techniques can be useful for simultaneous separation or purification of various kinds of process contaminants such as cell debris, host proteins or aggregates (SWIETNICKI, 2006). One promising example of a recently published method variant highly specialized on the improvement of refolding yields is the urea-gradient size-exclusion chromatography, which will be described in details in the succeeding section 2.3.1.

2.3.1 Refolding via Size-Exclusion Chromatography

The underlying principle of group separation gel filtration is made use of to realize the required exchange between denaturant and refolding-promoting conditions: A packed bed consisting of approximately spherical particulate beads, which are ideally chemically inert, forms a porous matrix. The internal porous system of the beads is theoretically only accessible for solute molecules smaller than the given exclusion limit of the considered medium, e.g. salts or, as in this case, denaturants. Low molecular weight components steadily diffuse in and out the porous system and are thereby delayed in their passage down the column. On the contrary, solute molecules larger than the exclusion limit have access to the extraparticular volume, frequently termed V_0, only. Hence, these molecules pass through the column faster and elute first, followed by other components in order of decreasing size (JANSON, 2011).

For conventional SEC refolding approaches, the column is usually equilibrated with renaturation buffer at first. Afterwards, the sample of denatured and reduced protein is injected and driven through the column under continuous flow. Excluded from the porous system at least in parts or even completely, target protein molecules migrate from the denaturing loading buffer into refolding conditions, following the size-exclusion principle explained above.

The understanding of the role of SEC media as refolding-improving matrices was predominantly characterized by the suggestion that the unfolded protein molecules are physically isolated within the porous system of the gel, comparable to the cage effect. According to this assumption, the molecule separation suppresses the tendency of unfolded polypeptide chains to aggregate in free aqueous solution, which can be regarded as a countermeasure of thermodynamic systems to the exposure of hydrophobic residues buried otherwise inside the tertiary structure of the native conformation. The reduction in the probability of two protein molecules to meet one another during the solvent exchange process would therefore contribute to the correct refolding as individual monomers (DING et al., 2011; SU et al., 2011).

Apart from this basic theory of SEC matrix functionality in protein renaturation, there is strong evidence for a different mode of action when applying gel chromatography column systems for refolding purposes: It was shown in distinct approaches by DING et al. (2011) as well as the cited reference work (WILMS, 2010) that the use of simple desalting materials may be superior to high resolution fractionation gels for renaturation attempts. Experimental results reproducibly led to higher refolding yields when denatured and reduced hen egg-white lysozyme underwent the chromatographic buffer replacement procedure on Sephadex G-25 columns, thus, in a desalting matrix entirely restricting the access of protein molecules to the porous system. This observations refer to the comparison of Sephadex G-25 to various protein fractionation SEC media, like Superdex 200, Sephacryl S-100 and S-200, with exclusion limits above the target protein's molecular weight, allowing the molecules to diffuse in and out the porous system. Subsequently, it has been concluded that effective – in some cases even most effective – protein refolding may take place in the interstitial volume of an SEC column only.

Whether or not a molecule is excluded from the porous system of a SEC medium depends on the material's pore size distribution as well as the hydrodynamic radius and shape of the considered molecule. In terms of the applied Sephadex G-25 medium the nominal exclusion limit is 5 kDa for globular proteins according to the manufacturer, hence, it most likely prevents all of the proteins used in the presented work (14.3-18.3 kDa) from access to the porous volume.

2.3.2 Refolding via Urea-Gradient SEC

A significant improvement, as SU et al. (2011) call it, to this standard refolding procedure is the additional application of a denaturant gradient. A gradually decreasing linear gradient of the urea (or guanidine hydrochloride) concentration is initially formed at the end of column equilibration, just before the denatured sample is loaded. Subsequently, protein molecules pass through the continuously changing urea environment until finally reaching 100 % renaturation buffer (see figure 2-4). This strategy, consecutively referred to as urea-gradient SEC, aims at a smooth transition in the buffer replacement process, thereby suppressing the frequently observed spontaneous misfolding and aggregation of polypeptide chains facing harsh conditional changes (GU et al., 2001; LI et al., 2004; WANG & CHENG, 2010).

Besides the introduction of a gradient-wise buffer transition, which was a key upgrade to the basic SEC renaturation procedure, there exist several more modifications of the solvent exchange principle. These include dual gradient techniques, like combined denaturant and pH or *L*-arginine gradient, as well as a continuous annular strategy, where aggregated or misfolded intermediates are separated within a long column path and may afterwards be recycled to improve final product yield. Another alteration to standard gradient SEC is the so called chaperone solvent plug technique, where a small volume of denaturant buffer is applied right before and after sample loading to avoid direct contact of unfolded proteins with refolding buffer and, thus, suppress aggregate formation (SU et al., 2011).

All of these upgrade strategies involve further efforts on hardware, know-how and optimization and are motivated by a potential benefit for very specific refolding tasks. The actual enhancement to the renaturation effectiveness as well as feasibility in principle must be tested and confirmed for every individual case. Although refolding capability and efficacy must, of course, be validated for simple urea-gradient based SEC renaturation, too, this technique is generally of less instrumental

complexity and commonly enables comparably facile adaption to different target proteins (GU et al., 2001; GU et al., 2002, LI et al. 2004).

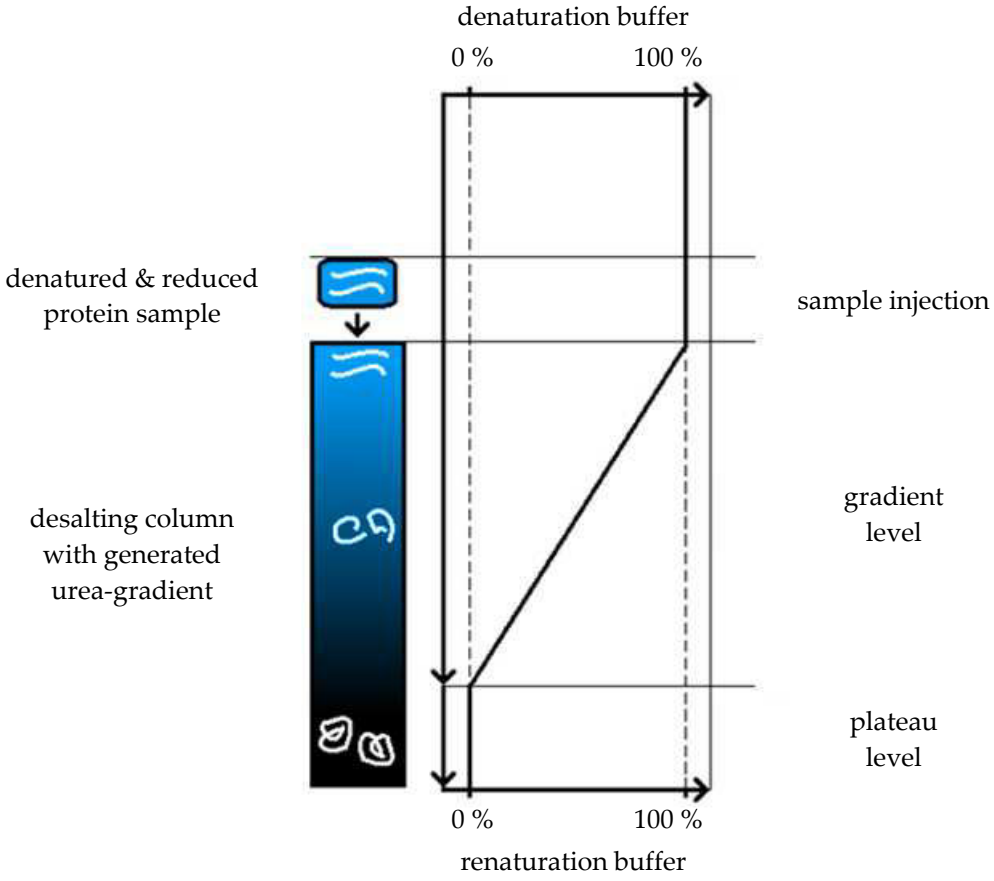

Fig. 2-4: Methodic concept of a urea-gradient size-exclusion chromatography illustrated schematically. After equilibration of the SEC column with refolding-promoting buffer conditions a gradient step with increasing concentration of denaturation buffer is applied. Subsequently, the denatured protein sample is injected and eluted by 100 % denaturation buffer. The principle of size-exclusion drives the protein through the column with greater velocity than the surrounding solvent molecules, thus, the protein migrates through the gradient until being eluted in 100 %renaturation buffer.

2.4 Protein Analysis by Fluorescence Spectrometry

2.4.1 Phenomenon of Fluorescence

By definition, luminescence is the occurrence of light emission from any kind of substance subsequent to energetic excitation. Two categories of luminescence can formally be distinguished, fluorescence and phosphorescence, dependent on the character of the excited state. The energy transitions between excitation and emission is typically illustrated by a Jabloński diagram as presented in figure 2-5. However, the time delay from excitation to emission of phosphorescence is slow (milliseconds to seconds) and its occurrence in general is rare. Thus, its practical use for analysis is rather limited. The more common and comparatively more rapid (about 10 nanoseconds) phenomenon of fluorescence is of high relevance for photometric analysis in biosciences and will therefore be discussed in some more details in the succeeding sections. A substance, which is able to absorb light energy of a specific wavelength and re-emit light of lower energy, so of longer wavelength, is termed a fluorophore.

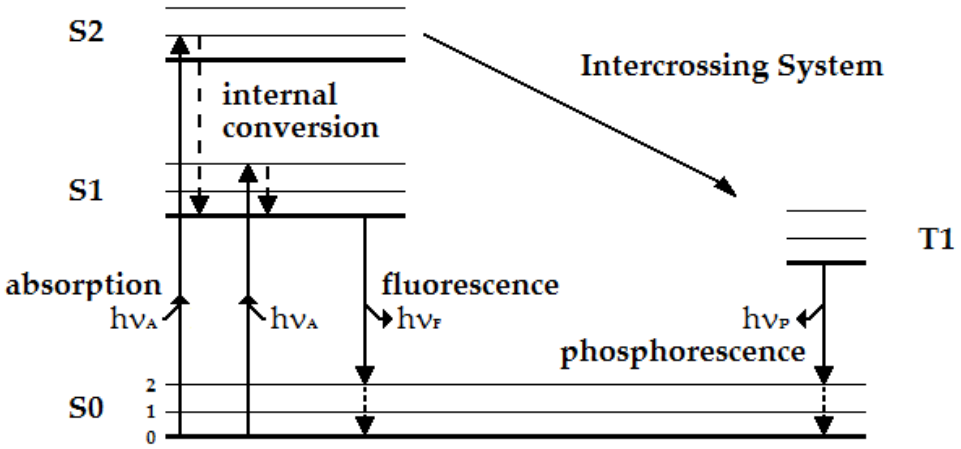

Fig. 2-5: Typical representation of a Jabloński diagram. Each of the electronic states, i.e. singlet ground state (S0), first singlet state (S1), second singlet state (S2) and first triplet state (T1), subdivides into a number of vibrational levels (0, 1, 2, etc.). Internal conversions are marked with dashed lines (- - -), while interorbital energy transfer is encoded by solid lines (—). (modified after ROUESSAC & ROUESSAC, 2007)

After absorption of light energy, an electron from a fluorophore's singlet ground state (S0) is excited to some higher vibrational level of either S1 or S2, which represent the first and second singlet electronic states of the molecule, respectively. Thereafter, usually a rapid relaxation to the lowest vibrational level of S1 takes place. This is termed an internal conversion and is generally completed within 10^{-12} seconds or less after excitation. This means, since total fluorescence lifetimes are typically about 10^{-8} seconds, internal conversions are usually finished prior to emission. Thus, it can be approximated that fluorescence emission commences from an equilibrium excitation state, i.e. the lowest vibrational energy state of S1. The high-energy state of the excited electron at S1 is still thermodynamically unfavorable. Due to this, the electron drops down to the highest vibrational level of the ground state S0 and the energy difference is equalized by the emission of light, the fluorescence.

A so called Stokes shift to a higher wavelength, but to lower energy, is subsequently observed between absorption and emission spectra. The internal conversion of absorbed energy to the lowest vibrational level of S1 is one major cause for the reduced energy of emitted light. Moreover, electrons from S1 typically decay to higher vibrational states of S0, followed by an additional internal conversion of the excess vibrational energy to heat instead of light emission. Although these are the main impacts on Stokes shifts, fluorophores can display further wavelength offsets caused by excited-state reactivity, energy transfer between fluorophores, complex formation as well as solvent effects (LAKOWICZ, 1999).

2.4.2 Protein Fluorescence

For the purpose of protein analysis, fluorescence spectrometry is widely used to provide valuable information on the structure and conformational changes of the target macromolecule. Moreover, concentration and purity are typical sample characteristics derivable from fluorescence data to a certain extent.

It is typically aromatic groups, which contribute to the fluorescence of biomolecules. Their system of delocalized pi electrons provides absorptive properties, which is a basic prerequisite for energy uptake and transition, thus, fluorescence. Among the 20 proteinogenic amino acids, only tryptophan (Trp), tyrosine (Tyr) and phenylalanine (Phe) possess aromatic groups. Hence, these amino acids are frequently termed intrinsic fluorophores of proteins. A first short view on their respective spectra of absorbed light intensities (see figure 2-6) elucidates that the indole group of tryptophan is by far the most predominant fluorophore. Nevertheless, general interpretation of spectroscopic data from fluorescent samples becomes increasingly complex with the number of fluorophores contributing to the resulting emission spectrum.

Phenylalanine has hardly any influence on total fluorescence of a protein additionally containing tryptophan and/or tyrosine residues, owing to its minor quantum yield, i.e. the amount of photons emitted per photon absorbed (LONGWORTH, 1981). Furthermore, typically performed excitation at wavelengths above 280 nm prevents phenylalanine from being excited at all. In a similar manner, one can diminish the influence of tyrosine fluorescence to a great extent, when the excitation wavelength is greater than 295 nm. However, even if excitation is done near the absorption maximum of tyrosine at 274 nm, radiation-free energy transfer to tryptophan residues as well as general interaction of tyrosine with the peptide chain reduce the fluorescence intensity referring to tyrosine effectively.

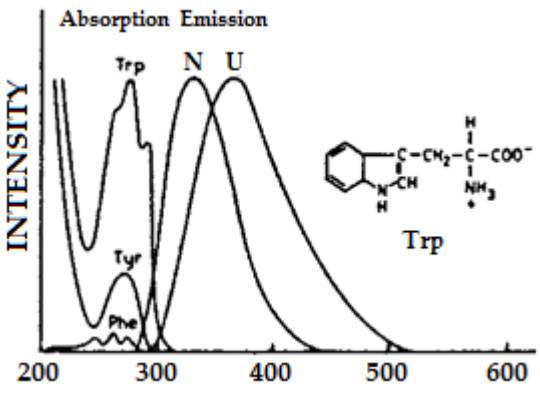

Fig. 2-6: Illustration of a shift in the fluorescence spectrum of a tryptophan residue induced by unfolding of a protein and the resulting exposure of the intrinsic fluorophore to the aqueous solvent phase. The x-coordinate shows absorption and emission wavelengths in nanometers, while the y-coordinate represents emission fluorescence intensity in arbitrary units. Labels N and U mark the spectra of native and unfolded protein state, respectively. (modified from LAKOWICZ, 1999)

Apart from internal energy conversion, the Stokes shift of tryptophan is especially sensitive to surrounding solvent conditions. In aqueous solutions and pure form, an indole group absorbs light near 280 nm and emits light at about 340 nm, but the emission wavelength is highly sensitive to solvent polarity changes. A blue shift to shorter wavelengths may occur for tryptophan residues buried within a natively folded protein conformation, while the emission maximum may be red-shifted if the protein is unfolded and tryptophan residues are extensively exposed to the aqueous surrounding (see figure 2-6). In addition to the solvent-dependent shift in the emission wavelength, frequently a change in fluorescence intensity is observed as well. Buried within the intact three-dimensional polypeptide structure, tryptophan is shielded from surrounding molecules, which can suppress or enhance fluorescence intensity. A decrease of so called quenching effects can occur if the protein unfolds and, hence, the fluorescence signal would be intensified. But unfolding may lead to reduced emission intensities as well, especially in cases where the fluorophore is then easier accessible for quenching solvent component. A closer look at quenching effects is given in the succeeding section.

2.4.3 Quenching Effects

Quenching in terms of fluorescence spectrometry generally describes the diminishing of detectable fluorescence intensity due to various influences. When the excited-state fluorophore is deactivated upon contact with some other molecule in solution, the occurrence is referred to as collisional or dynamic quenching and the deactivating molecule is named a quencher. Halogens, heavy atoms, acrylamide or oxygen may all act as quenchers, yet the exact mechanism of interaction varies with the fluorophore-quencher pair. The decrease in fluorescence intensity probably occurs due to electron transfer, spin-orbit coupling or intersystem crossing to the triplet state (see figure 2-5) between such pairs. Besides this diffusion-dependent molecular collision phenomenon, quenchers may form non-fluorescent complexes with

fluorophores. This process is frequently termed static quenching as it can already occur in the energetic ground state.

Regarding the macromolecular level of proteins, a common quenching effect is mediated through ligand binding, when quencher molecules come into close spatial proximity of one or more intrinsic fluorophores.

Both, dynamic as well as static quenching mechanisms require direct molecular contact between the quencher and fluorophore. However, some non-molecular effects may cause signal quenching, too. For example, optical properties of the sample, such as turbidity or high optical densities, are trivial but frequently observed reasons for reduced fluorescence intensities (LAKOWICZ, 1999).

Molecules in solution absorbing near either the excitation or emission wavelength maximum also quench the measurable fluorescence intensity. Concerning the first case, if excitation energy is partly taken up from quenchers, the aromatic amino acids within the protein are shielded against being reached to full extent by the excitation light. Thus, the quantum yield of the fluorophore is reduced proportionally. In the second case, when light emitted by the fluorophore is absorbed by quenching molecules, the quantum yield theoretically remains the same as for unquenched solutions. But fluorescence intensity does not reach the detector entirely, thus, analytic results are adulterate.

Internal conversions as introduced in the preceding sections may also be considered as quenching effects. Especially at high analyte concentrations, the conversion of absorbed light energy into vibrational and thermal energy decreases the fluorescence intensity. The quenching impact of alterations in the solvent polarity surrounding a fluorophore has also been mentioned above.

One last non-molecular quenching effect, which should be referred to in this summary, is the influence of temperature. The relative fluorescence intensity of tryptophan itself is reduced at rates of 1-2 % per degree when the solution temperature rises (see figure 2-7, A). As part of the macromolecular construct of a protein, such rates may be subject to slight variations, yet, the general rule of a

negative impact of increasing temperatures on measurable intensities still appears to be valid. Even when the protein sample solution is heated markedly above room temperature (i.e. > 25 °C or 298 K), these rates are approximately constant at 1-3 % per degree, until finally reaching a protein-specific thermal denaturation temperature range altering the slope (see figure 2-7, B and C) (BÖHM, 2005; SAINI & DEEP, 2010).

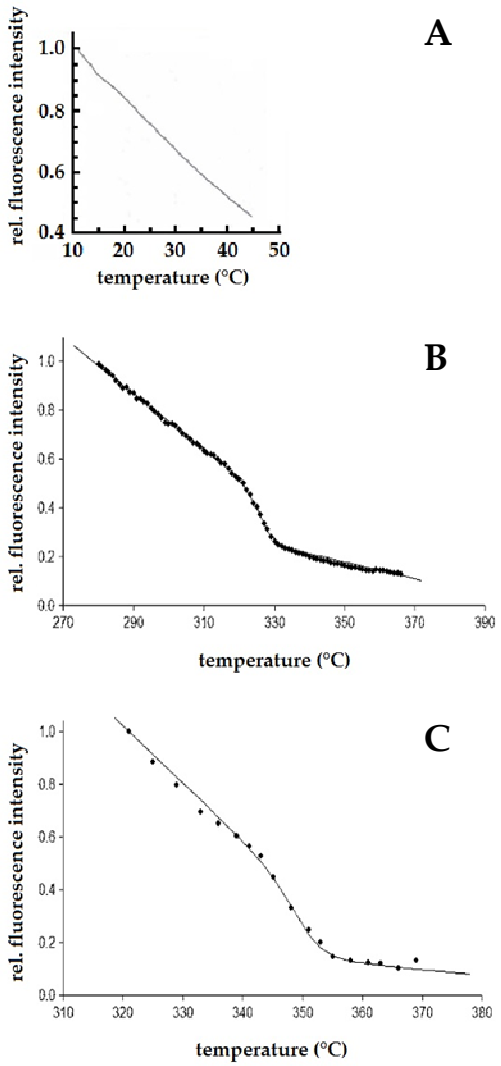

Fig. 2-7: The effect of temperature on the fluorescence intensity of tryptophan (**A**) was investigated using a solution 1 µM Trp. Excitation was done at 278 nm and detection of fluorescence emission at 355 nm. Within the observed range the measurable intensity decreased linearly with rising temperature (modified after BÖHM, 2005).

Integrated within the three-dimensional structure of trypsin (**B**) or lysozyme (**C**) the thermally dependent loss of fluorescence intensity is still observable, though the decrease per degree varies slightly. Excitation was performed at 295 nm, while emission was followed at protein-specific maximum, i.e. 345 and 334 nm, respectively (modified after SAINI & DEEP, 2010).

2.4.4 Signal phenomena in Fluorescence Spectra

Commonly, interference of fluorescence measurements is due to scattered or stray light as well as ample impurities. Two related artifacts which are frequently observed in fluorescence spectra are the so called Rayleigh (Tyndall) peaks on the one hand, and Raman bands on the other hand.

The first phenomenon is an effect caused by the solvent in which the fluorescent analyte is dissolved. A certain fraction of excitation light is often absorbed and immediately re-emitted in all directions at the same wavelength by solvent compounds. The extent of Rayleigh scattering is generally dependent on the polarizability of the solvent. A considerable intensification of the signal at excitation wavelength may occur in the presence of non-dissolved particulates, such as protein precipitates. This light scattering effect is sometimes referred to as Tyndall scattering (ZUMDAHL & ZUMDAHL; 2008)

Moreover, during the Rayleigh scattering process a small portion of the incident light can be converted into vibrational and rotational energy. This results in a weak emission of light with lower energy relative to the excitation radiation. Raman bands are typically 100 to 1000 times less intense than Rayleigh peaks. The energy difference between absorbed and re-emitted photons is independent from incident light energy and therefore the signal occurs at a constant wavelength for each solvent.

Finally, light diffraction caused by the monochromator gratings of higher orders results in the appearance of scattering bands at every multiple of the excitation wavelength. A summary on these commonly observed signal effects is given in figure 2-8.

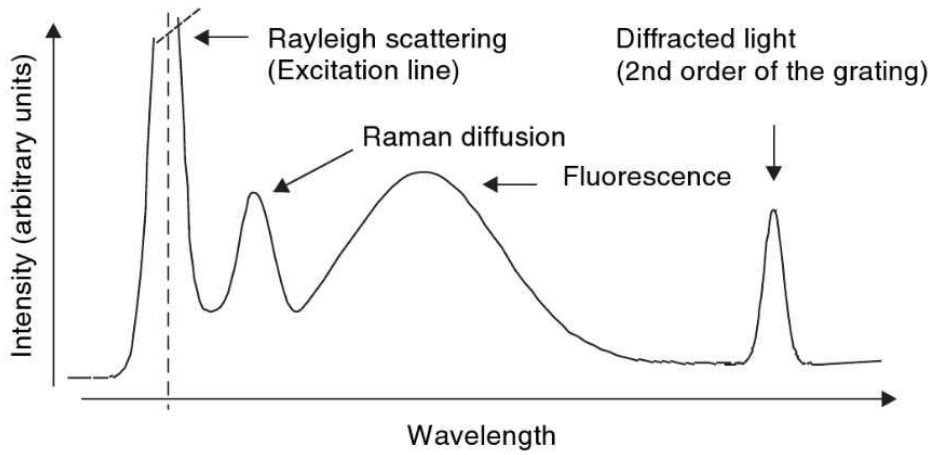

Fig. 2-8: Characteristic fluorescence spectrum illustrating typically observed intensity peaks. Rayleigh and Raman bands as well as stray light effects are typical phenomena which occur in addition to the actual analyte signal (ROUESSAC & ROUESSAC, 2007).

Especially in case of protein analysis, the wavelengths of excitation and emission are frequently close together, separated by only a few dozens of nanometers. Therefore, the occurrence of Raman and Rayleigh peaks may define the limit of detection as it is governed by the ability to distinguish analyte fluorescence from these solvent interferences (LAKOWICZ, 1999; ROUESSAC & ROUESSAC, 2007).

2.5 Test Proteins

2.5.1 Lysozyme from Hen Egg-White

Lysozyme is an enzyme classified as mucopeptide *N*-acetylmuramoylhydrolase (E.C. 3.2.1.17). It catalyzes the hydrolytic cleavage of β-1,4-glycosidic linkages between *N*-acetylmuramic acid and *N*-acetyl-*D*-glucosamine residues present in the Gram-positive mucopolysaccharide cell wall and is therefore in some cases called a muramidase. In general, the enzyme is a colorless, sweet tasting protein and its strong antimicrobial activity originated both, its incidental discovery by Sir Alexander Fleming in 1922 as well as its subsequent naming. There exist several different types of lysozyme with minor amino acid variations in their primary sequence (IRWIN et al., 2011).

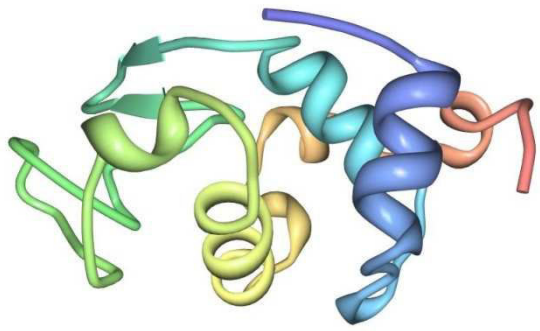

Fig. 2-9: Hen egg-white lysozyme structure illustrated by a ribbon model modified from Protein Data Bank (PDB) entry 1LZC, which is based on experimental data of MAENAKA et al. (1995).

The hen egg-white lysozyme (HEWL) used for the presented experimental series belongs to the so called type c, indicating likewise either that it was found in and isolated from chicken for the first time or that it is the most frequently observed (conventional) type of lysozyme throughout all living organisms.

HEWL is a basic protein with an isoelectric point near 11.0 and consists of 129 amino acids leading to a molecular weight of 14,388 Da. Its tertiary structure includes several α-helices and β-sheets and can be subdivided into two domains, in-between of which a cavity is formed representing the catalytic site (see figure 2-9). Four disulfide bonds build structure-stabilizing linkages in the native conformation and their reduction results in loss of bioactivity and even the sweet taste (MASUDA et al., 2001). Moreover, HEWL contains six tryptophan residues at positions

28, 62, 63, 108, 111 and 123, each of which contributing differently to the fluorescence spectrum of the natively folded conformation. At neutral pH in aqueous solution the enzyme emits light with highest intensity at a wavelength near 341 nm. During denaturation, tryptophans usually buried within the tertiary structure become exposed to the surrounding aqueous phase and a solvent-dependent wavelength shift to about 353 nm is frequently observed (IMOTO et al., 1971; FORMOSO & FORSTER, 1975).

2.5.2 α-Lactalbumin from Bovine Milk

α-Lactalbumin (alpha-LA) is a whey protein expressed in the lactating glands of all mammals at typical concentrations of 0.6-1.7 g/L. The protein is a regulatory component of lactose synthase. Via reversible protein-protein interaction it modulates the affinity of the catalytic constituent UDP-galactose β-*N*-acetylclucosaminide β-1,4-galactosytransferase I for different acceptor substrates (KRONMAN et al., 1981; EIGEL et al., 1984).

Bovine alpha-LA is a globular metalloprotein of 14,175 Da and possesses distinct binding sites for calcium, zinc and some other metal ions. The binding of Ca^{2+} is assumed to be a major structure-stabilizing factor for the native conformation and to play a decisive role in the regeneration of native-like alpha-LA from the reduced, denatured state. Alpha-LA from cow's milk consists of a single polypeptide chain of 123 amino acids including four disulfide bonds and four tryptophan residues, the latter of which are located at identical positions relative to HEWL apart from the missing Trp62 and Trp111 (FORMOSO & FORSTER, 1976; VEPRINTSEV et al., 1997; CHRYSINA et al., 2000).

Obviously, the protein structure is closely related to c-type lysozyme, with about 40 % amino acid identity and an extraordinary similarity of the three-dimensional appearance (see figure 2-10). Both proteins most probably evolved from a common

ancestral protein (McKenzie & White, 1991). At the same time, alpha-LA provides a characteristic example of dramatic functional divergence in homologous proteins.

Not only physiological activity and binding potentials, but also some basic physico-chemical properties are markedly different. Alpha-LA, for example, is an acidic protein with an isoelectric point (pI) of 4.5, while the net charge of HEWL on the contrary is balanced to zero at a pI of around 11.0.

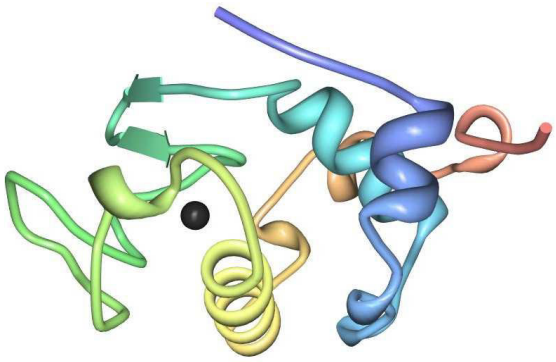

Fig. 2-10: Ribbon-based structure of bovine α-lactalbumin binding a Ca^{2+} ion (black sphere). The image has been modified from PDB entry 1HFZ and uses structural data form Pike et al., 1996. The structural similarities to HEWL are most likely due to a common evolutionary origin.

One property of alpha-LA worth mentioning concerning its refolding behavior is the formation of a stable molten globule intermediate state upon exposure to mild denaturing conditions or during refolding. This intermediate form is reported to possess compact three-dimensional structure, intact secondary structure elements, but lacking native-like packing interactions of amino acid residues (Kuwajima, 1996).

2.5.3 β-Lactoglobulin B from Bovine Milk

Bovine β-lactoglobulin (beta-LG) is the major whey protein of cow's milk found at concentrations of 2-3 g/L, which makes up about 45-50 % of total whey protein content (Eigel et al., 1984). At physiologic conditions beta-LG exists in dimeric form, whereof each monomer consists of a single chain of 162 amino acids. Several genetic variants of beta-LG can be distinguished, deviating from one another in minor amino acid changes. Two variants, namely A and B, are most prominent in bovine milk and occur in almost equal shares (Mulvihill & Donovan, 1987). Both forms differ from each other in the amino acid sequence at positions 64 (A → Asp; B → Gly) and 118

(A → Val; B → Ala). However, even these minimal alterations yield distinct biologic and physicochemical properties of each variant regarding their solubility, heat and pH stability as well as self association characteristics. For the presented work, only the B variant was used in order to limit the study of refolding behavior to a single type. Subsequently, if not explicitly specified, the term beta-LG refers to the genetic variant B of bovine β-lactoglobulin. For this variant a molecular weight of 18,276 Da can be calculated from the specific amino acid content (TOWNEND, 1964; OLIVEIRA et al., 2001).

Concluding from its three-dimensional structure and primary sequence, beta-LG belongs to the lipocalin family. Most members of this protein superfamily are characterized as transporters of small hydrophobic molecules, such as triglycerides, fatty acids as well as aromatic hydrocarbons and retinols (KONTOPIDIS et al., 2004).

The amino acid sequence of monomeric beta-LG comprises five cysteines, four of which are involved in the formation of two intramolecular disulfide bonds between residues Cys66-Cys160 and Cys106-Cys119 (VERHEUL et al., 1999). One single thiol group of Cys121 remains free and reactive, whereby its reactivity is reported to be highly dependent on solvent conditions, especially on the pH value (BUROVA et al., 1998; DIVSALAR et al., 2006). Moreover, beta-LG contains a total of two tryptophan residues. In the native structure, Trp19 is buried inside the molecule, while Trp61 is located close to a mobile surface loop between two β-strands (ARAI et al., 1998). In aqueous solutions kept at room temperature in a pH range between 5.5 and 7.5 beta-LG normally exists in dimeric form, which is stabilized via intersubunit salt bridges between Arg40 and Asp33 as well as four to eight hydrogen bonds (see figure 2-11). Near its pI of 5.1 the protein associates to octamers, while below pH 3.5 disassociation into monomers occurs due to the increase in repulsive surface net charge. Alkaline conditions above pH 7.5 promote monomerization, too. However, salt concentration may reduce ionic effects and increase dimer stability under extreme pH conditions. In addition to that, one has to consider that besides the

points above-mentioned the association behavior of proteins is a temperature-dependent process (GOTTSCHALK et al., 2003; NAQVI et al., 2010).

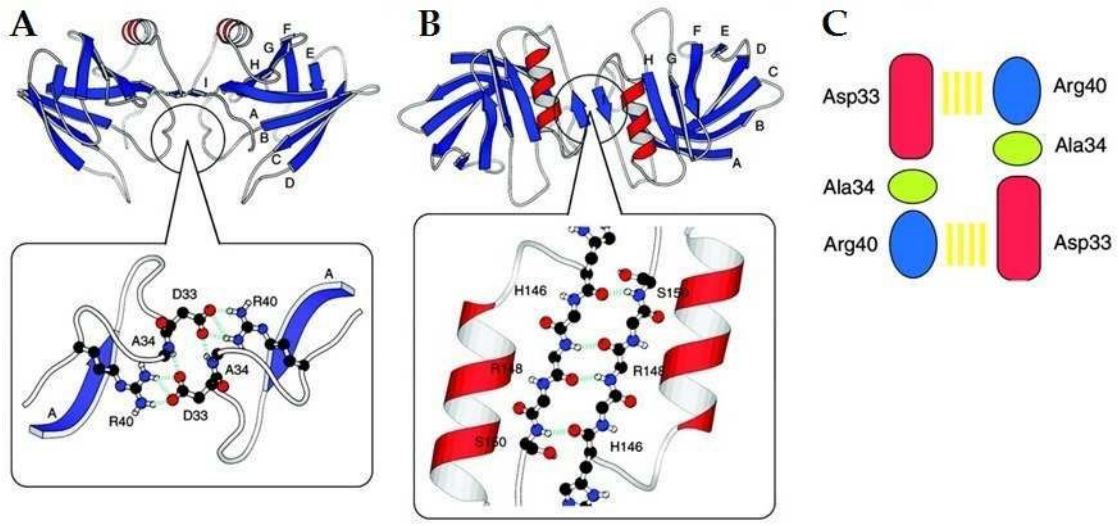

Fig. 2-11: Structure of dimeric β-lactoglobulin created from X-ray data using PDB code 1BEB. All nine secondary structure β-strands are labeled alphabetically (A-I). With respect to the I-strand (**A**) shows a side view and (**B**) a top view on the dimer interface. The corresponding magnified cutouts indicate hydrogen bond positioning. A schematic representation of intermolecular salt bridges is given in (**C**). (modified after SAKURAI & GOTO, 2002)

3. Materials and Methods

3.1 Materials

3.1.1 Reagents and Chemicals

Tab. 3-1: Chemicals and reagents used for refolding experiments and analytics.

Substance	Supplier
Calcium chloride, 99.9 % p.a. ($CaCl_2$)	Merck, Darmstadt
1,4-Dithiothreit, ≥ 99 % p.a. (DTT)	Roth, Karlsruhe
L-Glutathione reduced, ≥ 98 % (GSH)	Merck, Darmstadt
Glutathione oxidized, ≥ 98 % (GSSG)	Roth, Karlsruhe
α-Lactalbumin, Type I, ≥ 85 %, from bovine milk, Lot# 110M7003V	Sigma, Steinheim
β-Lactoglobulin B, ≥ 90 %, from bovine milk, Lot# 048K7003V	Sigma, Steinheim
Lysozyme, EC 3.2.1.17, from chicken egg white, ≥ 30.000 FIP-U/mg, Lot# K40776381 042	Merck, Darmstadt
Micrococcus lysodeikticus, ATCC No. 4698	Sigma, Steinheim
Potassium dihydrogen phosphate, ≥ 99,5 % p.a. (KH_2PO_4)	Merck, Darmstadt
Sodium chloride, ≥ 99.5 % p.a. (NaCl)	Roth, Karlsruhe
Tris(hydroxymethyl)aminomethane, ≥ 99 % (TRIS)	Fluka, Mannheim
Urea, ≥ 99,5 % p.a.	Roth, Karlsruhe

3.1.2 Equipment and Software

Tab. 3-2: Utilized electronic laboratory equipment and related control software.

Equipment	Supplier	Control Software
ÄKTA purifier UPC 100 Liquid Chromatography System	GE Healthcare	Unicorn 5.2
BioLogic DuoFlow Liquid Chromatography System	Bio-Rad	BioLogic DuoFlow System Software 4.0
RF-5301 PC Spectrofluorophotometer	Shimadzu	Panorama Fluorescence 2.1
Ultrospec 2100 pro UV Spectrophotometer	Amersham Bioscience	SWIFT II

3.1.3 Buffer solutions

All given information on masses to be weighed refer to the preparation of one liter (1 L) of each buffer solution. Buffers utilized for liquid chromatography experiments were degassed after preparation via vacuum filtration by repeated suctioning over a cellulose acetate membrane (Sartorius Stedim Biotech) with a pore size of 0.45 μm. To avoid microbial growth in general and especially to prevent the process from potentially corruptive impacts by ongoing oxidation of some buffer components, all solutions were consumed or otherwise replaced after a period of 3-5 days.

Tab. 3-3: Buffer solution D – Denaturation buffer.

Ingredient	Concentration (mol/L)	Molar mass (g/mol)	Mass (g)
Urea	8.00	60.06	480.48
TRIS	0.10	121.14	12.11
NaCl	0.20	58.44	11.69
DTT	0.03	154.20	4.63

Tab. 3-4: Buffer solution R^+ – Renaturation buffer *including* glutathione.

Ingredient	Concentration (mol/L)	Molar mass (g/mol)	Mass (g)
Urea	2.00	60.06	120.12
TRIS	0.10	121.14	12.11
NaCl	0.20	58.44	11.69
GSH	0.0060	307.33	1.84
GSSG	0.0006	612.60	0.37

Tab. 3-5: Buffer solution R^- – Renaturation buffer *without* glutathione.

Ingredient	Concentration (mol/L)	Molar mass (g/mol)	Mass (g)
Urea	2.00	60.06	120.12
TRIS	0.10	121.14	12.11
NaCl	0.20	58.44	11.69

As a special explanatory note it must be mentioned that the molar urea concentrations in buffers D and R^+ were subject to variations in case of the DoE approach referred to in section 3.2.3.1.

The pH values of buffers D and R^+/R^- were adjusted with 1 M hydrochloride to the desired value, whilst taking into account the preferential pH range of the target protein as well as the pH-dependence of oxido-shuffling agents GSH/GSSH (see table 3-6).

Tab. 3-6: Overview on protein specific buffer pH values.

Sample Protein	Buffer pH
HEWL	8.5
alpha-LA	8.0
beta-LG	8.0

For all refolding experiments, it was distinguished between renaturation buffers either containing (R^+) or free of (R^-) glutathione in oxidized and reduced form. In terms of alpha-LA an additional ingredient was needed: Calcium chloride ($CaCl_2$) in a molar concentration of 1 mM was added due to the Ca^{2+}-related stability dependence of the protein (see section 2.5.2).

Moreover, all chosen pH values were deduced from stability data and literature and were meant to provide an appropriate protein-specific, renaturation-promoting environment. The addition of 0.2 M sodium chloride to all chromatography-related buffer solutions was intended to suppress non-specific interactions between proteins and the stationary phase surface.

Tab. 3-7: Buffer solution A – Lysozyme assay buffer.

Ingredient	Concentration (mol/L)	Molar mass (g/mol)	Mass (g)
KH_2PO_4	0.066	136.09	8.98

The preparation of buffer A was done according to a protocol described in DIRKSEN (2010). With a 1 M solution of sodium hydroxide the solution pH was adjusted to 6.2, as recommended by the supplier (Sigma, Steinheim) for a *M. lysodeikticus*-based lysozyme assay.

3.1.4 Column and Medium for SEC-Refolding

The chromatographic desalting resin Sephadex G-25 (Medium quality) was used as stationary phase for all SEC-refolding experiments. This material consists of beads made of dextran cross-linked via epichlorhydrine. Particle size distribution ranges from about 85 to 260 µm and its pore size distribution leads to a nominal fractionation range from 1.000 to 5.000 Da for globular proteins according to manufacturer's data.

The chromatographic medium was manually packed into a C 10/40 column (GE Healthcare, Uppsala) with a final bed height of 37.5 cm leading to a total column volume (CV) of about 29.5 mL. Though this type of column is dedicated for the application of pressure up to 1 bar (0.1 MPa), empirical data showed a reproducible stability up to 3.5 bar (0.35 MPa) without visible changes in the chromatographic bed height.

3.2 Methods

3.2.1 Fluorescence Spectrometry

A two-dimensional fluorescence spectrometry analysis was performed with all chromatographic fractions showing an UV absorption signal during gradient SEC refolding of alpha-LA and beta-LG. Analysis was done on a "RF-5301 PC Spectrofluorophotometer" from Shimadzu, Duisburg, controlled by the corresponding software "Panorama Fluorescence 2.1" including a graphic evaluation tool. The photometer uses a xenon lamp (150 W) as light source and a photomultiplier (R 3788-02) for detecting fluorescence emission at right angle relative to the excitation beam. An overview on instrument parameters and system values set as constants for all measurements is given in table 3-8.

Tab. 3-8: Standard fluorescence spectrophotometer parameters applied as default settings for all protein analysis experiments.

Measurement mode	2-D emission scan
Excitation wavelength	295 nm
Wavelengths of detection	Start: 285 nm Stop: 450 nm
Aperture slot	Excitation: 10 nm Emission: 10 nm
Measurement speed	super
Sensitivity	low

A precision quartz cuvette of type Suprasil 101-QS (Hellma, Jena) with an optical path of 10 mm was used as reaction cell for spectral analysis. For best reproducible results the sample volume should equal or exceed 2 mL in order to reduce potential refractivity effects by the upper liquid surface or air bubbles.

3.2.2 Denaturation of Proteins

Appropriate conditions regarding denaturation time and temperature were initially chosen according to literature data (DE BERNARDEZ CLARK, 1998; DIRKSEN, 2010; WANG et al., 2010; DING et al., 2011).

To allow continuous stirring, the minimum sample volume for all proteins was 2 mL. The required amount of lyophilisate was dependent on the final concentration and the type of protein, respectively. All samples were directly weighed into a small glass ware beaker or flask and brought to the desired volume using buffer solution D. Subsequently, the solutions were sealed with plastic paraffin film and incubated for about 4 hours on a magnetic stirrer through heating to approximately 35 °C while stirred at low speed. For the first couple of experiments the denaturation progress of each protein was examined at irregular intervals via activity assay (HEWL) and/or wavelength fluorescence spectrometry (all proteins). Prior to such testings or the final sample loading, all denatured and reduced protein solutions were allowed to cool to room temperature.

Although initially aiming at and tested for the complete unfolding and disulfide reduction of lysozyme, the conditions turned out to be suitable for proper denaturation of alpha-LA and beta-LG, too. Corresponding experimental data are given in section 4.1. The adequacy of equal denaturation conditions was partly deduced, on the one hand, from structural similarity between alpha-LA and HEWL. On the other hand, several publications (GALANI & OWUSU-APENTEN, 1999; HAMADA & DOBSON, 2002) report the maximum unfolding of beta-LG for 8 M urea likewise, even though the native protein shows its highest stability at the chosen incubation temperature of 35 °C (PACE, 1990).

3.2.3 Urea-Gradient Size-Exclusion-Chromatography

The standard liquid chromatography system used for all refolding experiments was an ÄKTA purifier UPC 100 system (GE Healthcare). Yet, a BioLogic DuoFlow system (Bio-Rad Laboratories) was used additionally for reproduction runs in order to principally rule out system- or pump-specific influences on the refolding success. An overview on the basic system component parts is given in table 3-9.

Tab. 3-9: Relevant standard items of utilized liquid chromatography systems.

	ÄKTA purifier UPC 100	BioLogic DuoFlow F10
Pump Heads	P-900 max. 100 mL/min	F10 max. 10 mL/min
Detectors	UV/Vis (path length: 2 mm), pH, conductivity	UV/ Vis (path length: 5 mm), pH, conductivity
Mixing Chamber	M-925 2 mL	MX-1 0.750 mL
Controller Unit	USB controller unit CU-950	USB bitbus communicator
Injection Valve	INV-907	ARV 7-3
Fraction Collector	F-920	BioFrac

Default mode of operation

Basically, all urea-gradient SEC experiments were conducted according to the general strategy described in the corresponding theoretical section 2.3.2. The term *default* experimental setting hereinafter refers to the following method configuration:

At first, an equilibration step with 100 % buffer solution R^+ containing 2 M urea ($c_{\mathrm{urea,R}}$) was performed within 2-3 column volumes (CVs) until stable conductivity and UV baselines were reached. Equilibration was then followed by a urea-gradient step over a length of 7.5 mL (l_{grad}) leading to a transition from 100 % renaturation to

100 % denaturation buffer D at a urea concentration of 8 M ($c_{\mathrm{urea,D}}$). This configuration was consistent with the original setup (WILMS, 2010) and defined the standard molar slope of the gradient (s_{grad}) as 0.8 M/mL according to equation 3-1.

$$s_{\mathrm{grad}} = \frac{c_{\mathrm{urea,D}} - c_{\mathrm{urea,R}}}{l_{\mathrm{grad}}} \qquad \text{Eq. (3-1)}$$

A 0.2 mL sample loop was used for loading and injection of denatured and reduced protein samples onto the column. Injection was done by flushing the sample loop with 0.6 mL of denaturation buffer immediately after the gradient generation was finished. The mobile phase used during and subsequent to sample injections was constantly held at 100 % denaturation buffer. This final part of the method will consecutively be termed as the *wash-out* or *elution* step, although the latter usually refers to adsorption chromatography techniques.

General remarks

It is important to point out that in revision of the mode of operation from the reference work (WILMS, 2010), a general decision was made to change the type of solvent used after sample injection from re- to denaturation buffer. This precautionary treatment of the system was intended to resolubilize and wash out potentially adherent aggregates which may have occurred during refolding experiments and possibly cause adverse effects in succeeding runs.
Furthermore, regardless of the particular urea concentration of any buffer solution used in the course of this work (see section 3.2.3.1), the molar slope of the gradient defined by equation 3-1 was kept constant in all experiments.

An overview on chromatographic parameters which were set as constant for the urea-gradient SEC refolding of all test proteins is provided in table 3-10.

Considering the total volume of about 45 mL (~ 1.5 CV) assigned to the applied final wash-out step, the approximate overall solvent consumption per run can be taken from table 3-11.

Tab. 3-10: Chromatographic default settings applied for the urea-gradient SEC refolding of all proteins of interest.

Volumetric Flow Rate (mL/min)	0.2 *)
Sample Volume (mL)	0.2
Fractionation Volume (mL)	3.0
UV Detection Wavelength (nm)	280

*) Apart from the given value, experimental runs concerning the DoE approach referred to in section 3.2.3.1 were conducted at an elevated flow rate of 1.0 mL/min.

Tab. 3-11: Overall and proportional approximate solvent consumption of buffer solutions D and R for a urea-gradient SEC refolding run with default experimental settings.

	Default Vol. (CV)	**Buffer Solution D (mL)**	**Buffer Solution R (mL)**
Equilibration	3.0	0	90
Gradient	0.25	3.75	3.75
Wash-out	1.5	45	0
Total	**4.75**	**48.75**	**93.75**

Experimental outlook

In a first series of chromatographic runs a Design of Experiments (DoE) approach was carried out aiming at the optimization of urea concentrations in de- and renaturation buffers and the gradient length in between of these.

Secondly, the consumption of some particular buffer components was subject to further optimization attempts in order to enhance the overall cost efficiency of urea-gradient SEC lysozyme refolding. Both of these two method improvement strategies were conducted using lysozyme, as the refolding behavior of this model protein is well-studied and was investigated several times before in the run-up of this work.

After successful establishment of such an advanced method, additional efforts were made to transfer the improved procedure to the renaturation of other test proteins, i.e. alpha-LA, beta-LG.

Roughly summarized one could state that the default settings explained above were subject to various changes in the course of the presented work. The context of these modifications is described in details in the succeeding subsections.

3.2.3.1 Gradient Optimization by Design of Experiments

The term Design of Experiments (DoE) refers to a methodology regarding the planning and statistical evaluation of experimental series. The general aim of DoE is using as few experiments as possible to yield as much information as possible about the influence of process inputs on the resulting output. When successfully performed, this approach enables statistically significant conclusions on input-output interactions and allows quantitative description of their dependencies. Typically, DoE approaches are conducted in up to three steps. Firstly, the significance of influential factors is examined during a series of *screening* tests. Afterwards, statistically significant factors are subject to an *optimization* procedure aiming at spotting a range of desired output results. Finally, *robustness testing* is applied to mark narrow limits of parameter variation within which reproducibility of outputs is assured to a certain degree (SIEBERTZ et al., 2010).

For this work, two parameters were selected for optimization by using strategic planning following DoE. Through varying the molarity of urea in both denaturation (D) and renaturation (R^+) buffer it was intended to ideally make out and specify a downsized partition of the chaotrope gradient which is minimally required for adequate refolding of lysozyme (HEWL). Here, adequate meant leading to refolding yields comparable to what was already achieved through urea-gradient SEC renaturation of HEWL before, i.e. yields of active protein > 80 % (GU, 2001; WILMS, 2010).

Due to the fact that the chosen urea concentrations of both, de- (D) and renaturation (R^+) buffer, were already tested and repeatedly found to meet the requirements of effective and reproducible urea-gradient-based lysozyme refolding on SEC columns (WILMS, 2010; GU et al., 2001; GU et al., 2002; Li et al., 2002), the initial screening step was skipped.

Instead, an optimization DoE was planned as a two-dimensional, central composite circumscribed design (CCC) with both concentrations ($c_{\mathrm{urea,D}}$ and $c_{\mathrm{urea,R}}$) as inputs and total mass recovery (w) calculated from lysozyme activity as output. The predefinition of the range of urea concentrations to be investigated was primarily deduced from literature. GU et al. (2001) proposed a molarity of 2 M in refolding buffers for the renaturation of lysozyme. Most references, including TIMASHEFF & XIE (2003), suggest high molar urea concentrations of about 8 M for denaturation, however, little seems to be known about the necessity to start the renaturation-related buffer exchange from these high molarities.

A center point (CP) was chosen at 2 M urea in refolding buffer R^+ and 7.0 M in denaturation buffer D. The maximum deviations from this CP were specified as ± 0.7 M urea for R^+ and ± 1.4 M, which corresponds to a radius of $\sqrt{2}$ in the normalized circumscribed design, which is illustrated in figure 3-1. The correlation between relative coordinates and absolute urea molarities is additionally provided in the accompanying table 3-12.

As explained before, a molar gradient slope of 0.8 M/mL was predefined by the default experimental setting for urea-gradient SEC. Thus, for all chosen DoE parameter sets and the involved buffer-dependent alterations of urea molarity, the length of the gradient had to be adjusted in order to meet this criterion.

Moreover, the DoE approach was carried out following a full factorial design, which implies that none of the experiments represented in figure 3-1 is left out. This leads to a total of eleven runs including a triple determination of center point (CP) experiments, which provide a measure of process stability and variability.

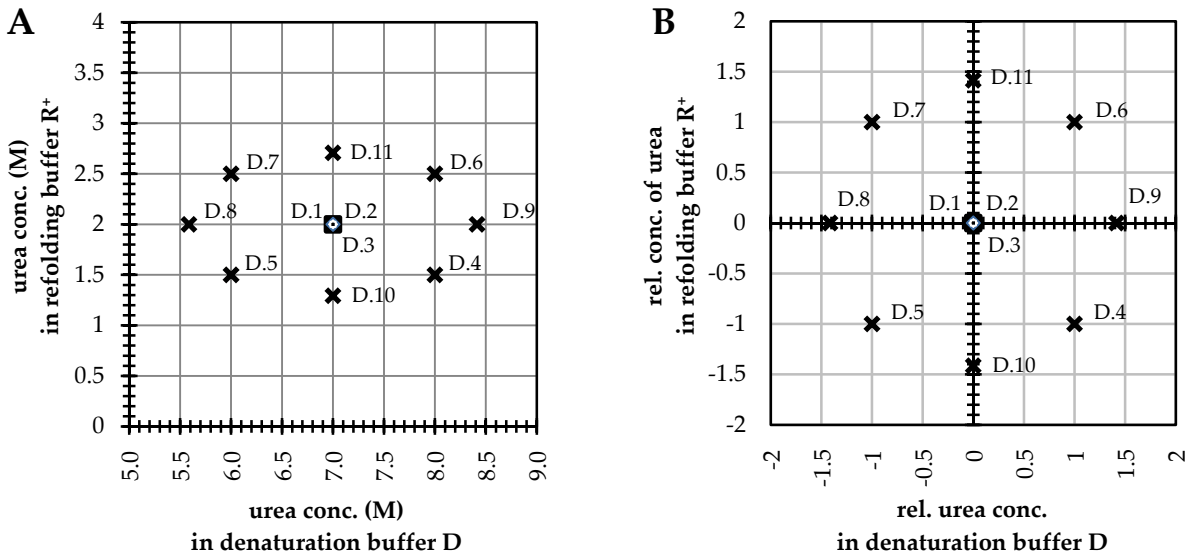

Fig. 3-1: Two-dimensional DoE layouts illustrating the absolute values (**A**) and normalized coordinates (**B**) of all parameter sets tested. Three center point (CP) experiments are indicated by (overlapping) filled squares at concentrations of 2 and 7 M urea (**A**) or zero coordinates (**B**), respectively. Crosses circumferentially arranged around the CPs label the positions of all other parameter sets. In case of a CCC design, these sets are located at a fixed radius of $\sqrt{2}$ in a normalized plot.

Tab. 3-12: Overview on relative and absolute values of all parameters sets of urea concentration in de- (D) and renaturation (R^+) buffers used for the DoE approach.

Exp. No.	Relative Coordinates		Urea Molarities (M)		Gradient Length *) (mL)
	D	R^+	D	R^+	
1-3 (CP)	0	0	7	2	6.25
D.4	+1	-1	8	1.5	8.13
D.5	-1	-1	6	1.5	5.63
D.6	+1	+1	8	2.5	6.88
D.7	-1	+1	6	2.5	4.38
D.8	-1.41	0	5.6	2	4.50
D.9	+1.41	0	8.4	2	8.00
D.10	0	-1.41	7	1.3	7.13
D.11	0	+1.41	7	2.7	5.38

*) Due to the technical capabilities of the ÄKTA purifier UPC 100 pump system, the actually programmed gradient length had to be rounded to two decimal places.

3.2.3.2 Development of an Advanced Mode of Operation

Another key objective of this work was to improve the urea-gradient SEC refolding in terms of overall process costs. All expenditures for laboratory equipment (e.g. electronic devices, quartz cuvettes), consumables (e.g. acid/base, gloves, paper tissues, PMMA cuvettes) as well as the basic supply of electricity, air and water were considered as constant values and therefore not taken into account. Moreover, the total volume of buffer consumed for a complete method cycle of (re-)equilibration, gradient generation and sample run remained unchanged (see table 3-11), although this is likely to involve further optimization potential.

Instead, the efforts made in this part of the work aimed primarily at improving the consumption of decisively expensive solvent components, namely glutathione in its oxidized (GSSG) and reduced (GSH) forms. With respect to the assumed prices of all buffer ingredients (see section 3.2.4), these two candidates were expected to involve a promising potential for economic optimization. Moreover, as stated in the theoretical chapters, general concepts of protein refolding and its kinetics usually do not precisely declare at which state during the course of folding the interaction with an oxido-shuffling system is most helpful or even mandatory to assist proper renaturation of proteins containing disulfide bonds.

For the practical implementation the default method was altered, on the one hand, by exchanging the equilibration buffer R^+ with its glutathione-free counterpart R^-. And on the other hand, an additional manually operated 7-port injection valve (IV-7) was mounted on the ÄKTA system between the already existing injection valve INV-907 and the column inlet to enable targeted introduction of glutathione-enriched buffer to the process (for valve position setups see appendix 7.A).

The experiments were divided into two approaches allowing the injection of 2 mL or 5 mL of glutathione-containing buffer, respectively, by means of accordingly dimensioned sample loops. Both approaches involved a series of experiments covering different parts (injection sites) of the gradient. The consequently observed impacts on gradient formation with regard to length and shape are exemplified in

figure 3-2. Glutathione samples were prepared by adding 6 mM GSH and 0.6 mM GSSG to a buffer or buffer mixture, the composition of which was supposed to be similar to the assigned gradient part. The buffer composition of loaded glutathione samples in relation to the respective site of injection can be taken from table 3-13.

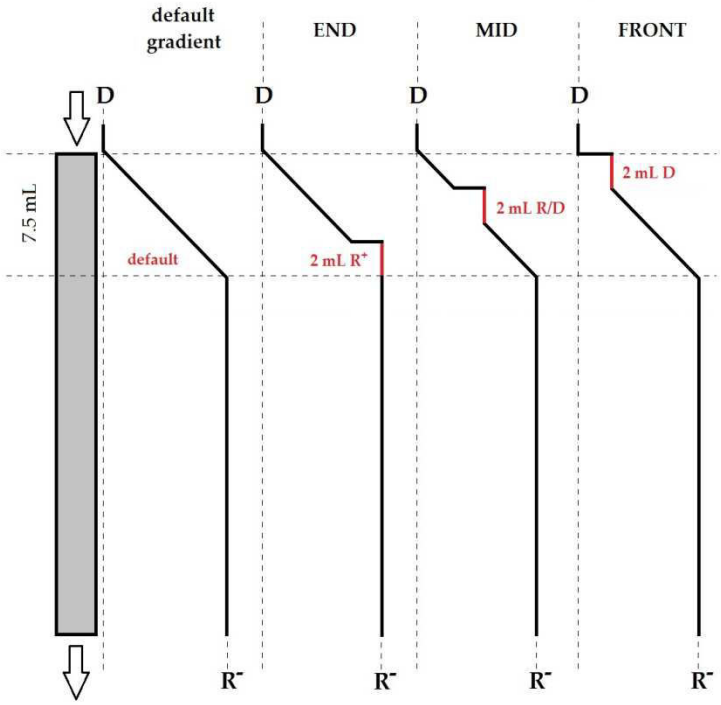

Fig. 3-2: Scheme illustrating the dependence of the overall gradient layout on the positioning of glutathione-enriched partitions (red) in comparison to the default setup, using a 2 mL sample as example. The terminology END, MID and FRONT refers to the location of the glutathione region relative to the flow direction through the column (arrows).
The oxido-shuffling system is injected during gradient formation in either 100 % refolding buffer (R^+), 100 % denaturation buffer (D) or a 1:1 mixture of both.

Tab. 3-13: Position of the glutathione-enriched buffer partition after gradient formation in relation to the flow direction (left column). Percentage of buffer variants A and B in glutathione sample buffer (right column).

Relative Position of Glutathione Sample	Buffer Composition	
	% D	% R
FRONT	100	0
MID	50	50
END	0	100

The injection valve IV-7 was switched back to load position immediately after its content (either 2 or 5 mL) was flushed onto the column. Thereby, the impacts of the additionally introduced sample loop on the pre-column dead volume and consequently on retention volumes were minimized. On the other hand, a part of the solvent gradient corresponding to the sample loop volume was enclosed within the loop, which led to a break in the linear transition of buffers D and R.
All runs involving the introduction of 2 mL of a glutathione-enriched buffer solution were conducted according to this approach, while its application was restricted to a reproduction run in case of the 5 mL addition.
Denatured and reduced samples of lysozyme (2.5 mg/mL) were used for the entire procedure of optimizing the glutathione consumption. All experiments were rated in terms of percent yield of active lysozyme. Reproduction runs were performed for conditions delivering best results within this criterion.

In case of a successful establishment of an advanced mode of operation, the ensuing goal was to achieve proper urea-gradient SEC refolding yields (in the magnitude of ≥ 80 % mass recovery) for new test proteins with only minor regulatory interferences. Therefore, denatured and reduced samples of alpha-LA and beta-LG were prepared at a concentration of 2.5 mg/mL under the denaturation conditions equal to those of HEWL (see section 3.2.2). These preparations were subsequently used as samples for the methodically most promising approach. Buffer components and pH values were adjusted as required according to the description in section 3.1.3.

3.2.4 Calculation of Protein-Specific Refolding Costs

According to the method description in section 3.2.3 the consumption of particular buffer components, namely reduced and oxidized glutathione (GSH/GSSG), was subject to major efforts aiming at the economic improvement of urea-gradient SEC protein refolding. To enable quantification of overall process costs and potential cost savings the underlying prices for all buffer ingredients are listed in table 3-14.

Tab. 3-14: Prices in euro per gram of all ingredients for buffer solutions D and R. The data is used for the calculation of specific costs and overall cost savings.

Index *i*	Buffer Ingredient	Price (€/g)
1	Urea	0,015
2	TRIS	0,100
3	NaCl	0,071
4	DTT	8,870
5	GSH	8,900
6	GSSG	18,400
7	$CaCl_2$	0,078

The pricing for all buffer components is consistent with WILMS (2010) and refers to comparably small packaging units purchased for laboratory scale experimental series. In terms of a process scale-up to pilot or production dimensions the individual prices per weight would be presumably lower.
Prices per milligram of HEWL, alpha-LA and beta-LG are derived from current supplier data and are approximately assumed as 0.01 €/mg, 1.00 €/mg and 2.25 €/mg, respectively.

With respect to buffer consumption per run (see table 3-11) and prices per gram of all buffer components from table 3-14 the fixed costs per run could be calculated from equation 3-2:

$$C_F = \sum (m_{ij} \cdot p_i) \qquad \text{Eq. (3-2)}$$

with:

i	-	buffer component *i*
j	-	type of buffer solution, with $j \in (D, R^+, R^-)$
C_F	-	fixed costs for buffer consumption (€)
m_{ij}	-	mass of component *i* in buffer *j*
p_i	-	price per gram of buffer component *i* (€/g)

Calculation of the total costs per renatured protein mass was done according to equation 3-3:

$$c_{tot} = \frac{C_F + p_P m_{PS}}{m_{PR}} = \frac{C_F + C_P}{m_{PR}} \qquad \text{Eq. (3-3)}$$

with:

c_{tot}	-	total mass-specific costs (€/mg)
C_F	-	fixed costs for buffer consumption (€)
C_P	-	costs of loaded protein mass (€)
p_P	-	price per milligram of protein (€/mg)
m_{PS}	-	mass of protein per sample (mg)
m_{PR}	-	mass of renatured protein (mg)

As a final remark, it should be emphasized that the above-mentioned alteration in eluting the protein samples with denaturation instead of renaturation buffer (see section 3.2.3) impinged on the overall and proportional buffer consumption relative to the reference work (WILMS, 2010). This is of decisive relevance regarding any comparison between both studies.

3.2.5 Quantification of Renatured Protein

3.2.5.1 Lysozyme Activity

A suspension of the Gram-positive bacterium *Micrococcus lysodeikticus* was used as substrate for the reaction mechanism of HEWL, as the enzyme catalyzes the hydrolytic disintegration of the stabilizing peptidoglycan scaffold enveloping the cell. The resulting degradation leads to a decrease in turbidity of a sample. The progress of cell lysis correlates with the enzyme activity and can be followed photometrically.

The following steps refer to an instruction protocol taken from DIRKSEN (2010) established for the measurement of HEWL enzyme activity on a milliliter scale:

Preparation of cell suspension at a concentration of 0.2 g/L:

8 mg *M. lysodeikticus* + 40 mL buffer solution A

Reaction batch:

990 µL cell suspension + 10 µL sample solution or blank

The utilized UV photometer Ultrospec 2100 pro (Amersham Biosciences) and the related control software enabled measurement of up to eight samples in parallel mode including a reference. Thus, mixing of sample (or buffer solution R^+ as blank) and cell suspension was done by aspiration and flushing out with a pipette immediately prior to starting each method run. All measurements were performed in disposable PMMA semi-micro cuvettes of 1.5 mL maximal volume and an optical path length of 10 mm. The decrease in turbidity was observed at a wavelength of 450 nm (A_{450}) over a period of 5.0 minutes. Dilution with buffer solution R^+ and re-measurement was carried out with all samples showing non-linearity in turbidity degression.

Using *M. lysodeikticus* as substrate, one unit (U) of enzymatic activity is defined as the amount of enzyme required to produce a change in A_{450} of 0.001 absorption units

(AU) per minute at pH 6.2 and 25 °C (SHUGAR, 1952). With respect to any dilution step activity can be calculated from equation 3-4:

$$\text{enzyme activity (U)} = \frac{\Delta A_{450}}{0.001}\ \text{min}^{-1} \cdot \text{dilution factor} \qquad \text{Eq. (3-4)}$$

As a rule of thumb, the cell suspension was regarded as being of acceptable quality when it possessed a UV absorption at 450 nm in the range of 0.800 to 1.000 AU.

3.2.5.2 Determination of Lysozyme Concentration

Triple determinations of the enzymatic activity of a freshly prepared 1 mg/mL lysozyme standard solution (buffer solution R^+) were performed on several test days. From the results an average factor was obtained, which allowed conversion between measured activity units and the mass concentration of actively folded lysozyme in an unknown sample.

3.2.5.3 Determination of Whey Protein Concentrations

Due to the lack of enzymatic activity, neither alpa-LA nor beta-LG concentration in solution can be determined through a specific assay. Hence, a different principle of measurement was made use of to provide qualitative and quantitative information on the target protein's folding state.

As explained in the chapters above, fluorescence spectrometry may be a valuable tool for protein analysis. Put in highly simplified terms, qualitative conclusions on folding state could be drawn from wavelength at maximum intensity (λ_{max}), while quantification is possible through absolute intensity values. In preliminary tests all proteins, including HEWL, were examined by fluorescence spectrometry to elucidate the respective λ_{max} in renaturation buffer R^+. These samples were assumed to represent the state of native conformation.

In order to determine the concentration of alpha-LA and beta-LG, for both of them a calibration series of at least 6 points was generated in the range of 0.016 to 0.50 mg/mL. Subsequently, the measured fluorescence intensities at λ_{max} were plotted in relation to their referring protein concentrations. Here as well, buffer solution R^+ was used for the preparation of all calibration solutions, as this equals best the expected solvent conditions within which renatured protein was most likely to elute from the chromatography column.

3.2.5.4 Calculation of Refolding Yield

Using the respective fraction volume (see table 3-10), as set in chromatographic methods, the protein mass was calculated for all samples from previously determined concentrations. The total refolding recovery of an experimental run is defined as the percent ratio between the sum of all individual masses per fraction and the total protein mass in the injected sample (see equation 3-5). The terms refolding yield or recovery as well as mass yield or recovery will hereinafter be used interchangeably.

$$w = \frac{\sum(c_k \cdot V_{frac})}{m_0} \cdot 100\ \% = \frac{\sum m_k}{m_0} \cdot 100\ \% \qquad \text{Eq. (3-5)}$$

Symbols and variables represent:

w	-	mass recovery (%)
c_k	-	concentration of renatured protein in fraction k (mg/mL)
V_{frac}	-	fraction volume (mL)
m_k	-	mass of renatured protein in fraction k (mg)
m_0	-	total protein mass in loaded sample (mg)

4. Results and Discussion

4.1 Preliminary Tests (Protein Renaturation)

4.1.1 Fundamental Fluorescence Analysis

In preliminary tests all proteins were examined by fluorescence spectrometry according to the protocol given in section 3.2.1 in order to establish a solid basis for the fluorimetric distinction of denatured from native protein states. For both conformational phases, the wavelength at maximum fluorescence intensity λ_{max} was investigated.

At first, to mimic an environmental condition equal to, or at least highly analogous to the solvent in which renatured protein samples elute during refolding runs, each protein was incubated at room temperature for 2 h at a concentration of 0.25 mg/mL in renaturation buffer containing glutathione (R^+). These samples and their respective fluorescence spectra were assumed to represent the native state.

Secondly, the typical fluorescence signal of the denatured and reduced conformation was determined. In order to achieve complete unfolding and disulfide-reduction, all test proteins used in later refolding experiments were treated according to the protocol given in section 3.2.2 and their fluorescence emission was monitored after 4 h of incubation in denaturation buffer D. For all proteins of interest, but particularly with regards to the whey proteins alpha-LA and beta-LG, the main criterion for deciding whether or not a protein is adequately unfolded was a stable and reproducible shift in λ_{max}.

Figure 4-1 illustrates typically occurring fluorescence spectra of all proteins in the native and unfolded conformation determined as described above. A summary of the protein-specific λ_{max} of both states is additionally presented in table 4-1.

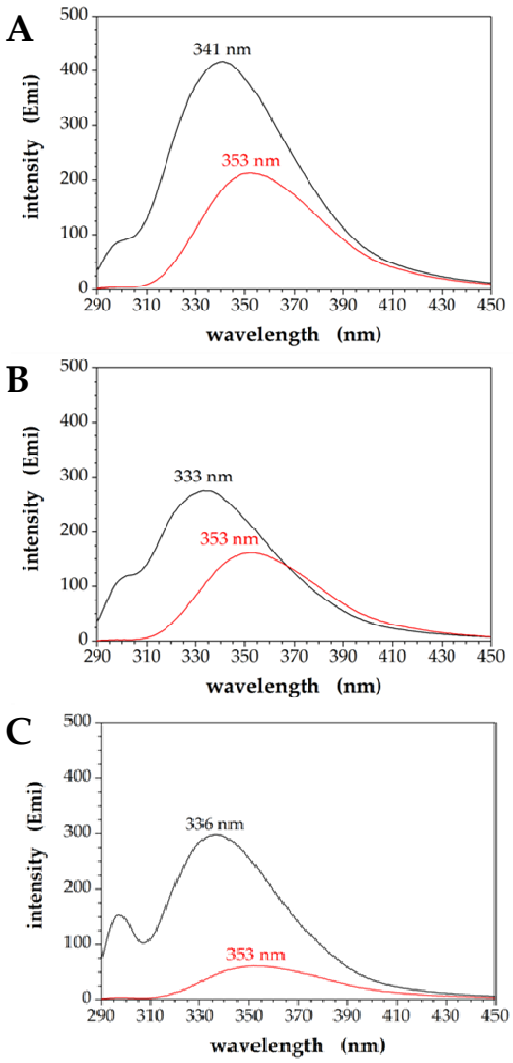

Fig. 4-1: Exemplary fluorescence spectra of native (black) as well as denatured and reduced (red) states of hen egg-white lysozyme (A), α-lactalbumin (B) and β-lactoglobulin (C). Incubation for approx. 2 hours in buffer solution R^+ at a protein concentration of 0.25 mg/mL served as standard conditions for the generation of all native samples. Denatured and reduced states were prepared by incubation in buffer solution D for 4 hours at about 35 °C. All samples were allowed to cool down to room temperature prior to spectrum analysis measurements. In order to restrict emission spectra to tryptophan signals only, excitation was done at 295 nm.

Tab. 4-1: Wavelength of maximum fluorescence intensity λ_{max} for the native and unfolded state of all test proteins.

	Native λ_{max} (nm)	Denatured and Reduced λ_{max} (nm)
HEWL	341	353
alpha-LA	333	353
beta-LG	336	353

Generally, in comparison of all proteins of interest the differences in the fluorescence intensity result from the unequal quantum yields of the intrinsic fluorophores and thereby reflect the accessibility of tryptophan residues for the excitation light in a given solvent environment. Apparently, the native states of alpha-LA (4 Trp) and beta-LG (2 Trp) yielded almost similar intensities. Thus, it is assumable that

lactalbumin tryptophans are buried deeper within the tertiary protein structure, while tryptophans of native β-lactoglobulin B possess comparably good access to excitation rays. The resulting fluorescence emission spectra may therefore have a high degree of similarity. Obviously, HEWL possesses the largest count of well-accessible tryptophans in buffer solution R^+ as its emission intensity was highest.

The apparently most remarkable element of this determination was the λ_{max} of 353 nm measured continuously for the denatured states of all proteins of interest. This value was known from previous HEWL experiments under comparable solvent conditions (DIRKSEN, 2010; WILMS, 2010) and represented, now as then, the completely unfolded protein state in which all tryptophan residues have maximum contact to the denaturing environment. Due to the fact that the same λ_{max} in tryptophan fluorescence was presently observed for alpha-LA and beta-LG, too, it is considered most likely that the chosen denaturation conditions were appropriate to entirely unfold these test proteins likewise (their tryptophan side chains were obviously exposed to an identical solvent surrounding).

The fluorescence intensities of the denatured protein conformations illustrate two solvent-dependent facts. On the one hand, in the completely unfolded state all tryptophan residues are evenly accessible for excitation rays, thus, a comparison of emission intensities basically mirrors the total amount of tryptophans in the respective amino acid sequence of each protein of interest. Yet, on the other hand, the absolute intensities were indisputably lower relative to the maximum emission of the respective native conformation. This indicates an intense quenching effect of the denaturant solvent solution, which is most probably caused by ground state interactions of the tryptophan indole ring and the thiol reagent DTT included in the denaturation buffer (SANYAL et al., 1989).

4.1.2 Calibration of Whey Protein Fluorescence Analysis

A second series of preliminary fluorescence experiments was carried out in order to enable protein quantification. Calibration curves were prepared for alpha-LA and beta-LG in the concentration range of 0.015 to 1.0 mg/mL. Analysis was carried out approximately two hours after preparation of the highest standard.

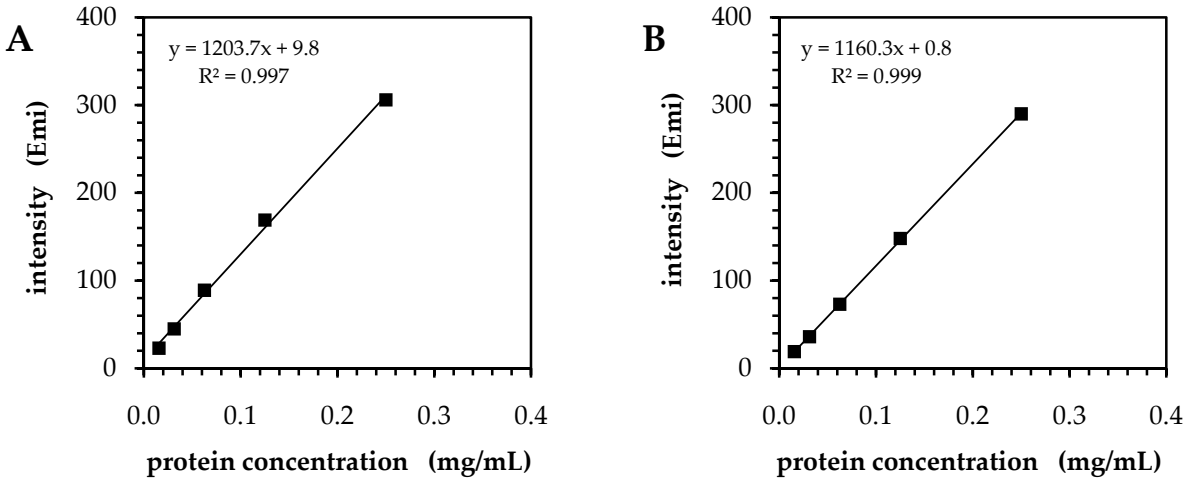

Fig. 4-2: Fluorimetric calibration curves of α-lactalbumin (**A**) and β-lactoglobulin (**B**) obtained in a concentration range of 0.015 to 0.25 mg/mL in renaturation buffer R^+. The given equation belongs to a linear regression trendline and R^2 indicates the respective coefficient of determination.

At protein concentrations in excess of 0.25 mg/mL, a non-linear interrelation with fluorescence intensity was observed, best described by a second order polynomial function. However, due to expectable protein concentrations in chromatographic samples, the range of evaluation was restricted to about 0.015 and 0.25 mg/mL. A best-fit curve based on linear regression was calculated by Microsoft Excel® 2007. The coefficient of determination R^2 was found to be ≥ 0.997 without exception, thereby providing a measure of accuracy of the trendline. By means of the generated calibration curves the concentration of each sample was elucidated by calculation from the linear regression equation given in the corresponding graphs in figure 4-2.

4.1.3 Lysozyme Activity

Preliminary experiments regarding lysozyme activity basically aimed at two different goals.

First of all, several standard solutions of 1.0 mg/mL HEWL in buffer R^+ were tested for bioactivity in triple determinations following the assay described in section 3.2.5.1. An overview on the outcome of this calibration experiment conducted on different dates is presented in table 4-2. According to these results, for the conversion between lysozyme activity and the concentration of actively folded protein a correlation of $1\ \text{mg/mL} \approx 74{,}500\ \text{U}$ was approximated for all later evaluations. While obtaining this conversion factor, maximum variations up to 4,000 U or 5.4 % were observed. These fluctuations were most likely induced by weighing inaccuracies, which are usually inevitable when handling small masses of freeze-dried, hygroscopic powder in the magnitude of only a few milligrams. Contributions from other experimental steps such as pipetting and dilution must be considered as further possible sources of error. The stated deviations must collectively be understood as a major uncertainty regarding final refolding yields calculated from these data.

Tab. 4-2: Experimental data from lysozyme activity measurements conducted on different days. The arithmetic mean used for all evaluations as a conversion factor between activity units and protein concentration is highlighted in bold type.

Activity (U)	Date of Experiment	Mean Activity (U)	abs. Deviation (U)	rel. Deviation (%)
75500	02.08.2012	**74500**	1000	1.3
71000	08.09.2011		- 3500	- 4.7
77000	02.11.2012		2500	3.4
70500	26.01.2012		- 4000	- 5.4
78500	27.01.2012		4000	5.4

Moreover, in addition to what was concluded from fluorescence data (see section 4.1.1), the progress of HEWL denaturation was investigated by performing activity assays in different time intervals during the denaturant incubation. Thereby, it was intended to confirm the expectable loss of enzymatic activity over time. An excerpt reflecting a typical course of measured residual activities is given in figure 4-3. It could be shown that a fast decrease in bioactivity was achieved following the elaborated denaturation protocol. Incubation times greater than 3 hours reproducibly led to a complete loss of enzymatic HEWL activity. Leaving a margin for conditional variations, an overall duration of 4 hours was therefore considered suitable for obtaining entirely denatured HEWL samples.

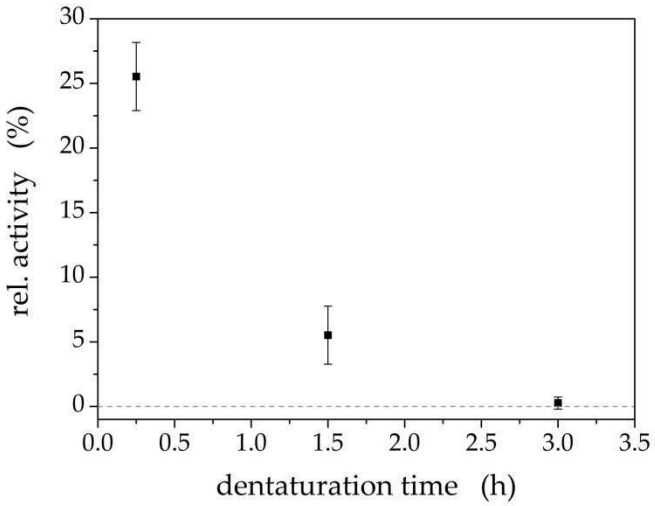

Fig. 4-3: Loss of relative lysozyme activity through incubation in buffer solution D at 35 °C. Samples (0.25 mg/mL) from three different preparations were examined over time. Error bars indicate the standard deviation from mean residual activities. In general, no significant activity was detectable after a total incubation duration of 3 h.

4.1.4 Default Urea-Gradient SEC Refolding Run

The experimental default setting is described in detail in section 3.2.3. In order to reproduce and confirm the successful application of this general procedure in comparison to the reference work, a series of standard experiments was carried out with HEWL at a concentration of 2.5 mg/mL. By taking the sample volume of 0.2 mL into consideration, this led to an overall protein mass of 0.5 mg loaded onto the column. The runs were usually preformed on the given ÄKTA purifier system at a flow rate of 0.2 mL/min. In consequence of this particular setup, a typical course of the UV absorption signal at 280 nm (A_{280}) as well as the conductivity in the resulting chromatogram is presented in figure 4-4.

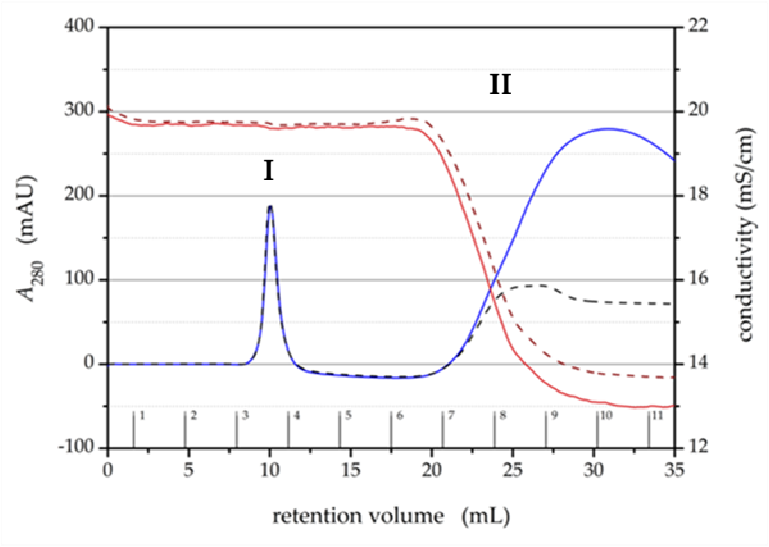

Fig. 4-4: Chromatographic standard profile of a urea-gradient SEC refolding run resulting from the default experimental settings. The experiment was performed on an ÄKTA purifier 100 system at a flow rate of 0.2 mL/min. UV absorption at 280 nm (A_{280}) is indicated by the blue line (V.1) and dashed black line (V.2), while the red (V.1) and dashed wine (V.2) curves represent the respective conductivity signals. Equilibration was done using refolding buffer R^+. A gradient from 2-8 M urea was created by progressively adding denaturation buffer D over a total volume of 7.5 mL and was followed by sample injection of 0.2 mL denatured and reduced HEWL at a concentration of 2.5 mg/mL. The region marked as (**I**) refers to the peak of refolded protein, while (**II**) represents the buffer transition in the gradient.

This standard profile comprised several repeatedly observed characteristics. First of all, the single UV peak marked as (I) could be identified as HEWL. With an emission λ_{max} at about 342 nm and mass recovery of about 85 % (calculated from enzymatic activity after 20 hours, see below) the efficient conformational reestablishment of biologically functioning lysozyme could be proven fluorimetrically as well as by activity analysis.

Concluding from the early stage of elution at a retention volume of 10.0 mL, one can assume that the peak eluted in 100 % renaturation buffer R^+ and in close proximity to V_0, representing the interstitial or void volume of the packed bed. For the exemplified default mode experiments V.1 and V.2 the peak area was reproducibly 225 mAU · mL, but typically ranged from about 215 to 240 mAU · mL in further reproductions.

Subsequent to a retention volume of around 19 mL a second UV peak (region II) reflected the linear buffer transition from R^+ to D, indicated by the reduction of conductivity from around 20 to 13-14 mS/cm and a simultaneous increase of UV absorption. GU et al. (2001) designated urea's generally non-ionic characteristics to be the main cause for decreasing conductivity with increasing denaturant concentration. Nevertheless, the interrelationship of conductivity (thus, resistance) and solution viscosity appeared to be a more sophisticated explanation. According to KAWAHARA & TANFORD (1966) the difference in relative viscosities between aqueous solutions containing 8 M and 2 M urea was observed about 1.5-fold due to intensified ion mobility restrictions. With possible contributions from thermodynamics or physico-chemical influences (e.g. temperature, pressure, other solvent compounds, etc.) in mind, this value strikingly fitted with the typical ratio of conductivities observed between buffer solutions D and R^+. A control experiment at least clarified that the phenomenon is predominantly governed by the difference in urea molarity (see appendix 7.B). However, the exact cause for the effect of changing conductivity with buffer transition might eventually remain unproven so far.

Notwithstanding, the contemporaneously observed change in UV absorption at 280 nm was unanimously reported to be owed mainly to the rise in the concentration of the low molecular weight component DTT (GU et al., 2001; GAO et al., 2003; LI et al., 2004). Following, an unequally expressed overshoot of the UV signal was recognized when comparing differently aged denaturation buffer solutions, most probably owing to the fast progressing oxidation of DTT thiol groups, for which half-lifes of about 1.5 hours have been reported (STEVENS et al., 1983). In case of a potential process upscale to industrial dimensions, solutions containing GSH or DTT are highly recommended to be freshly prepared on a daily basis in order to meet validation and consistency criteria. Nevertheless, in this work UV variability did obviously not significantly correlate with the method outcome in terms of refolding success and was therefore considered as a negligible phenomenon.

Typically, in between of the depicted partitions (I) and (II), approximately at 12.5 to 19 mL, a region of subzero UV absorption occurred. This decrease in A_{280} was probably owed to mixing effects of buffer solutions R and D as it was observable with or without any sample injection. Within the first milliliters of this intermediary region (fraction 6), weak HEWL activity was traceable in some cases. Yet, this observation lacked a clear tendency, but is most likely due to the tailing of peak (I) containing small amounts of refolded protein. Possibly, while folding back to a globular state, a certain (small) share of the HEWL molecules was able to penetrate into parts of the porous system. This would have temporarily retarded these molecules causing a slight right-sided expansion of the peak distribution. Statistic variances in the pore size distribution of the packed bed resin may occasionally emerge larger pores, which may potentially provide access to polypeptide chains of an unfolded protein – particularly when such oversized cavities appear close to the surface of the Sephadex beads.

The previous paragraphs summarized the appearance and major causes of recurrently observed phenomena for the default settings of urea-gradient SEC refolding experiments regarding HEWL on the given ÄKTA purifier system. High activity recoveries of refolded protein could be achieved using this setup.

However, a series of reproduction runs was carried out using the BioLogic DuoFlow system alternatively. The referring F10 pump system preferentially featured the low applied flow rate of 0.2 mL/min. An overlay of resulting exemplary chromatograms is presented in figure 4-5. Generally, the higher absolute signals, observable especially for the UV absorption at 280 nm, are likely to be explained by the greater path length (5 mm) of the analytical DuoFlow UV detection chamber (see table 3-9). The principally better congruence between conductivity and UV signals of the two runs relative to ÄKTA outcomes was assumed to result from carrying out the experiments in very close temporal succession. Thus, time-dependent buffer alterations were of minor influence.

As indicated by the sharper edging especially on the bottom part of the gradient, the reduced mixer volume and perhaps a different constructional layout of the DuoFlow system was obviously capable of realizing the gradient formation more adequately than the ÄKTA system. In reproduction experiments R.1 and R.2 moderately higher activity recoveries were achieved of 87.6 and 90.3 %, respectively. Hence, the improved conformity of the gradient step and the accompanying higher accuracy of the buffer transition apparently favored proper HEWL refolding.

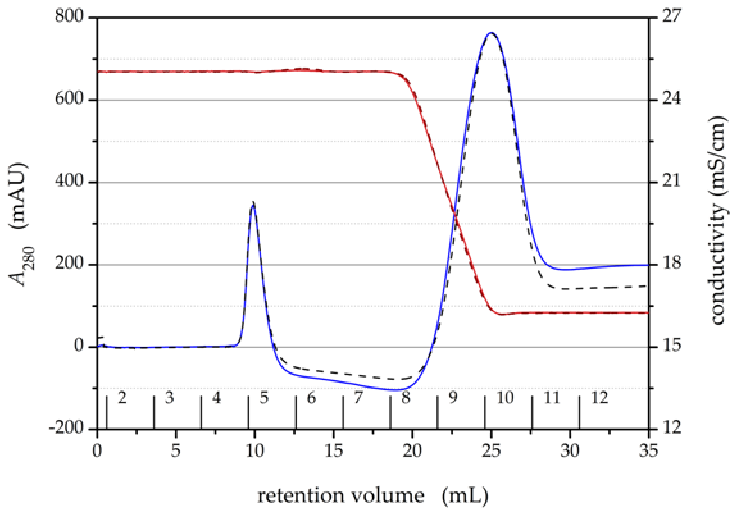

Fig. 4-5: Chromatographic profile of urea-gradient SEC reproduction runs for the refolding of HEWL. The reproductions were performed using default experimental settings on a BioLogic DuoFlow system at a flow rate of 0.2 mL/min. UV absorption at 280 nm (A_{280}) is indicated by the blue line (R.1) and dashed black line (R.2), while the red (R.1) and dashed wine (R.2) curves represent the respective conductivity signals.

According to equation 3-2 (see section 3.2.4), whilst taking into account the overall consumption of solvent solutions D (48.75 mL) and R^+ (93.75 mL), the costs per default mode run amounted to 2.45 € and 2.53 €, respectively, or 4.98 € in total.

Assuming the determined refolding yield of around 85 %, the mass-specific costs for HEWL refolding by default mode experiments were calculated by equation 3-3. According to this, 11.74 € accrue per milligram of renatured lysozyme. This value was considerably higher than what was observed in the reference work (7.86 €/mg). This is owed to two major reasons: First of all, the change in the process strategy (wash-out with solvent D, rather than R^+ in order to avoid/resolve on-column aggregate depositions) caused a difference in overall as well as proportional buffer consumption of solvents D and R^+, so that fixed costs per run had been reduced to about 4.50 € at that time. Moreover, with respect to equipment availability a 25 % larger sample volume (0.25 mL) was applied, which obviously did not adversely influence the overall protein recovery (~90 %) and was beneficial for the calculation of mass-specific expenditures.

Finally, time-related changes in activity measurements were examined in a supplementary test series concerning fraction samples from default runs V.1 and V.2. Figure 4-6 demonstrates the continuous development of HEWL activity recovery over a period of several hours until finally reaching a stable maximum. This phenomenon was assumed to be primarily based on the kinetics of disulfide-reshuffling to a conformational structure in which steric proximity facilitates thiol group interactions of cysteines. Perhaps, this intermediate state can be visualized as an already globular, yet swollen conformation that required further covalent linkages, such as disulfide bonds, for a final tightening step accompanied with the evolvement of maximum bioactivity.

With respect to the fact that specific folding kinetics and reaction rates are dependent on a variety of influences (e.g. protein concentration, ratio of GSH/GSSG, etc.), the tendency of the obtained results is in good agreement with recent findings from literature. WANG et al. (2009), for instance, observed best lysozyme activity recoveries (~90 %) for incubation periods greater or equal to 70 minutes subsequent to dilution refolding of lysozyme.

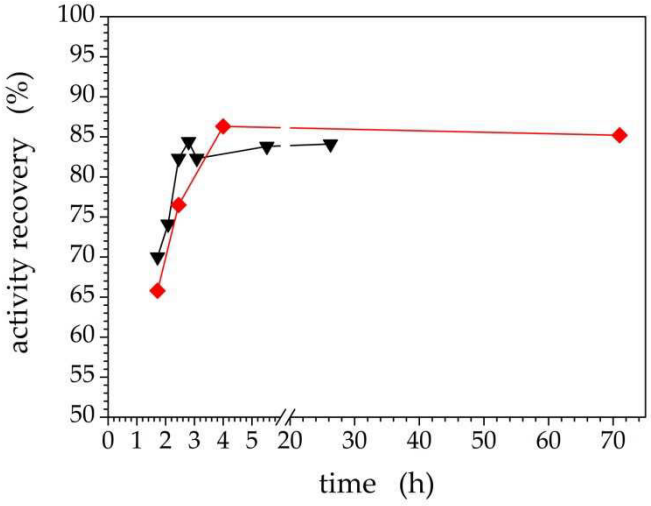

Fig. 4-6: HEWL activity of pooled fractions from urea-gradient SEC default runs V.1 (triangles) and V.2 (squares) was examined at irregular intervals. Several hours after sample collection from chromatography runs, constant activity recoveries were obtained and appeared to be stable for at least a couple of days.

A claim of decisive importance for subsequent experiments was deduced from the observation previously discussed: Unless specified otherwise, all quantitative statements hereinafter made regarding enzymatic activities refer to measurements carried out at least 20 hours after sample collection from urea-gradient SEC runs. By

following this analytic strategy the recently demanded incubation period needed for complete oxidative refolding was taken into account (see section 2.3). All fractionated samples were sealed with paraffin foil and stored at room temperature until analyzed in order to avoid alterations through external influences.

4.2 Gradient Adjustment through Design of Experiments

A DoE-oriented optimization of the buffer transition step was carried out in order to evaluate whether or not a certain partition of the urea gradient would be sufficient for proper refolding. The systematically planned strategy was done according to a central composite circumscribed design and all related experiments were performed at an elevated flow rate of 1 mL/min.

A summary of obtained results is provided in table 4-3 and depicted graphically in figure 4-7. Total activity recovery was considered as the measure of quantity to rate the respective refolding success achievable with each chosen parameter set.

In order to omit misunderstandings from the very beginning, it must be explicitly pointed out that all DoE experiments were carried out unintentionally neglecting the above mentioned incubation delay between sample collection and analytics. This was in fact owed to the circumstance that the DoE approach took place chronologically first, thereby unknowingly disregarding the later claimed way of proceeding.

Tab. 4-3: Overview on DoE outcome in terms of calculated activity recoveries. Brackets indicate results from reproduction runs.

Exp. No.	Relative Coordinates		Activity recovery (%)
	D	R^+	
1-3 (CP)	0	0	57, 37, 47 (33) (43)
D.4	+1	-1	42 (34)
D.5	-1	-1	45 (64)
D.6	+1	+1	60 (29) (33)
D.7	-1	+1	42 (77) (53)
D.8	-1.41	0	67
D.9	+1.41	0	41
D.10	0	-1.41	43
D.11	0	+1.41	37

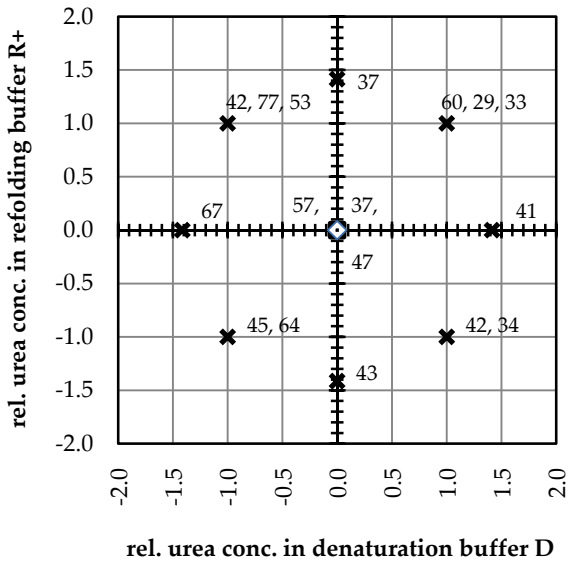

Fig. 4-7: Normalized CCC design diagram illustrating the outcome from all DoE experiments. The approach aimed at evaluating the impact of different gradient layouts regarding start and end level concentrations of urea.
Crosses mark the relative positions of chosen parameter sets and corresponding labels represent the measured activity recoveries in percent. Results of reproduction runs are separated by comma.

At the time of evaluation, the apparently most striking outcome of the experimental series was the evident inability to reproduce activity recoveries, even when applying identical conditions. In the following, this statement will be substantiated using the center point (CP) runs and two additional parameter sets as examples. However, from a general point of view, the obtained results indicated that the applied DoE approach lacked the ability to enhance the overall refolding efficiency.

In DoE approaches, results of CP experiments are usually considered the main criterion to rate the overall process stability and reproducibility. Figure 4-8 represents an overlay of three CP experiments (D.1-D.3), each one carried out on a different test date within one week using the same buffer solutions D and R^+. Room as well as reservoir solution temperatures were test-checked twice per day and did not fall below or rise above 21.5 to 24.0 °C, respectively. Thus, temperature-related effects were considered unlikely to have a significant impact on the refolding efficiency for the given experimental series.

Occurring variations of the UV signal in the gradient region were already addressed in the preceding section. Except these assumingly oxidation-based buffer fluctuations, the curve shapes of all signals – and particularly of conductivity courses – matched almost without noticeable divergences. Relative to the (ÄKTA system) default mode runs, the retention volumes of HEWL-related peaks were slightly

shifted to lower values between 9.56 and 9.73 mL. This might be explained by reduced non-specific interactions of the folding polypeptide chain and the solid matrix due to intensified convection under elevated flow conditions. At the same time, a moderate increase of the corresponding peak areas by around 10-15 % up to 260 mAU · mL was observed. The latter would principally strengthen the assumption of concomitantly enhanced activity recoveries, which could not be proven analytically, as outlined before.

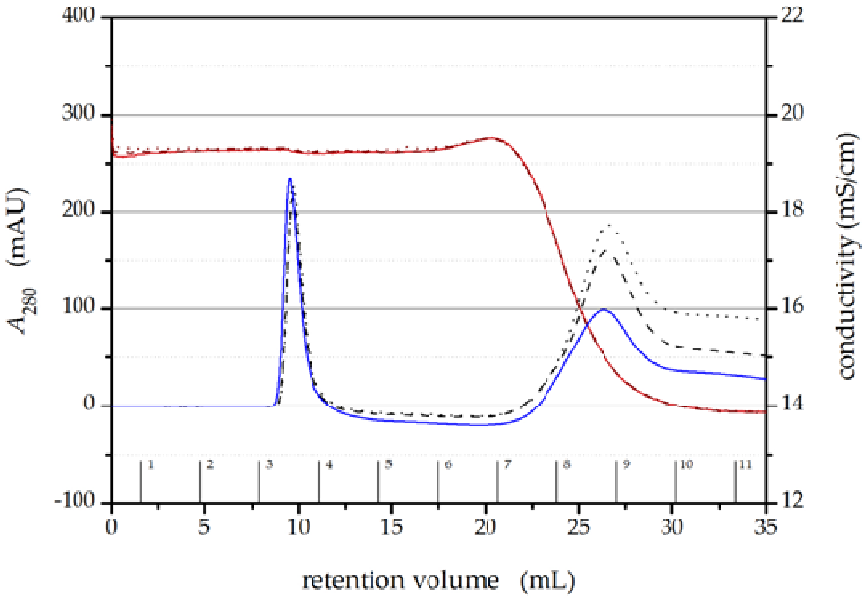

Fig. 4-8: Overlay chromatogram of DoE center point (CP) experiments. UV signals are indicated by solid blue line (D.1), dashed black line (D.2) and dotted black line (D.3), while conductivities are represented as solid red, dashed wine and dotted wine curves, respectively. Apart from the applied flow rate of 1.0 mL/min, all experiments were carried out under default mode conditions. The course of all monitored signals as well as peak characteristics strongly resembled the corresponding elements of the default chromatogram.

The chromatograms of DoE experiments D.6 and D.7 and corresponding reproductions as given in figure 4-9, are intended to additionally exemplify and emphasize the general validity of the observations made in the discussion of the CP runs. Just like then, apparently well-reproducible mass yields (deduced from peak area similarity) did not deliver activity recoveries of comparable uniformity. This

lack of continuity occurred throughout the entire series of DoE runs and was substantiated via reproductions on a random basis.

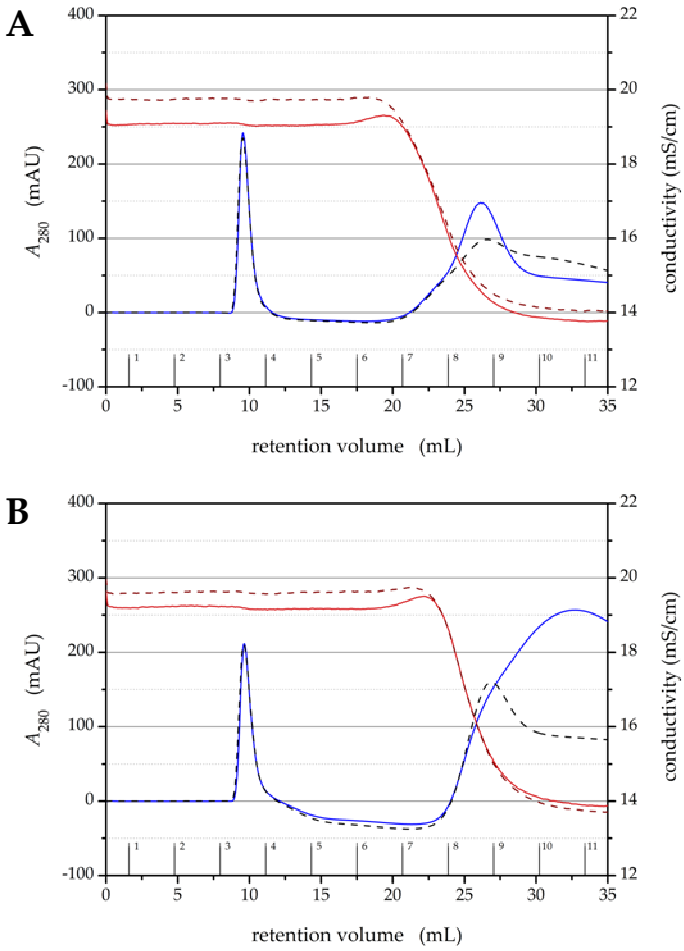

Fig. 4-9: Chromatograms of the DoE experiments D.6 (**A**) and D.7 (**B**) including corresponding reproduction runs. Solid lines indicate main runs, while repetition runs are indicated by dashed lines. Colors blue and black belong to UV absorption signals, while red and wine represent conductivity courses, respectively.
In principle, major elements as peak size and retention volume occurred similar to the default operation mode concerning urea-gradient SEC refolding of HEWL. Good congruence was observed for reproduction runs. However, referring measurable enzymatic activities were subject to significant variations.

However, despite this pronounced accordance of curve shapes as well as retention times and apparent peak areas, there was little consistency in measured activity recoveries (see table 4-3 and figure 4-7). Analytics were carried out roughly within approximately 1.5 to 4 hours after completion of each experimental run and the outcome was subject to considerable, yet undefined fluctuations. One fundamental reason concerning this variability of activity analysis may probably be found in performing the assay without paying precise attention to the time elapsed since collecting the respective samples. With respect to the later recognized significant changes in measurable activity within the first couple of hours after solvent exchange (see section 4.1.4), this way of proceeding must be taken as a major source of result falsifications. True values are likely to be higher, as the maximum activity was shown

to emerge in consequence of a prolonged incubation period of about 4 hours, allowing completion of folding and disulfide formation. The outcome of such defective analysis may therefore be qualified as being pre-mature. However, taking revisionary corrective actions was impracticable as the exact temporary context was untraceable in retrospective considerations.

Coincidently, the elevation of the applied flow rate turned out to be an unfortunate choice in general. Findings, made almost simultaneously to the discussed DoE procedure (by an associated working group), indicated irritations connected with the accelerated flow in the urea-gradient SEC refolding of HEWL using the identical system and column. On the one hand, increased mobile phase velocities (> 0.2 mL/min) generally yielded high activity recoveries of more than 80 % in default-like experiments, which pointed at a basically missing interdependency of theoretical plate height and refolding success under these conditions. On the other hand, similar to the recent observations, the reproducibility of activity recoveries seemed to be limited without elucidating a clear tendency or explanation. Perhaps, this was due to not taking into account the post-run time delay, either.

Subsumed from a rational point of view, it cannot be precluded in general that the planned DoE strategy itself might have been perfectly appropriate to examine the announced objective. In principle, this assumption was supported by the good overall reproducibility of chromatograms from main runs and repetitions.

Although unknowingly made misconceptions have to be admitted in terms of experimental setup (flow rate) and analysis (length and equality of incubation conditions prior to analytic measurements), the occurring variations might as well allow drawing another conclusion: Not all influential factors could have been taken into consideration in the first place – and especially potential parameter interactions have not been subject to profound examinations from the start. Intensified screenings enabling more precise statements on significant impacts and their interrelationships would be recommended in preparation of any method transfer to processes of industrial relevance.

However, protein refolding has repeatedly been shown to be highly sensitive to a very broad variety of influential factors. And as long as the exact influence of process variables is unknown (most probably owing to unrevealed system complexity, practical unfeasibility regarding instrumental equipment or efforts of time and labor) performing DoE optimization just by picking some few factors subjectively or at random is likely to fail. In terms of protein refolding approaches, significance and particularly interactions of most inputs is still unknown, which is apparently a consequence of the involved multidimensionality. Conducting remedial experiments remains vastly elaborate and is a case-by-case exercise due to protein-specificity of influence parameters. Thus, one probably has to admit that even a most sophisticated DoE approach may potentially be inapplicable in consideration of the multifaceted complexity of protein renaturation.

As the DoE experiments were chronologically conducted at an early stage of this study, the obtained results collectively questioned the overall basic capability of the chosen DoE strategy to yield information of general validity. At this particular point, when becoming aware of the fluctuations individually specified above, a decision was made to return back to a flow rate of 0.2 mL/min, which had repeatedly been proven to yield a reproducible success in HEWL refolding. Repetition of the developed DoE strategy under different flow conditions or with stronger focus on prior-to-analysis time delays would have been advisable, but was omitted with regards to overall time constraints of the project.

Instead, another challenging, yet promising objective was put focus on, namely to improve the established urea-gradient SEC default procedure in terms of economics.

4.3 Optimization of Glutathione Consumption

The experiments presented and discussed in the subsequent paragraphs aimed at gathering additional knowledge on the demand in glutathione for HEWL refolding, whereby the main focus was put on the optimization of the overall consumption of this costly oxido-shuffling compound.

Prior to the actual experimental series, a rough estimation was done in order to assess the minimum quantity of glutathione theoretically required to allow the reformation of all disulfide bonds (Dsb) per sample. Presuming an equimolar reaction between oxidized glutathione (GSSG) and the formation of a disulfide bond (see section 2.3), one can easily calculate the molar amount of GSSG needed to link all free cysteines of a given protein in principle.

The following considerations were based on the example of the default lysozyme sample:

$$m_{\mathrm{Lys}} = 2.5\,\mathrm{mg/mL} \cdot 0.2\,\mathrm{mL} = 0.5\,\mathrm{mg}$$

$$n_{\mathrm{Lys}} = \frac{m_{\mathrm{Lys}}}{M_{\mathrm{Lys}}} = \frac{0.0005}{14.388}\,\mathrm{mol} \approx 3.5 \cdot 10^{-8}\,\mathrm{mol}$$

Hen egg-white lysozyme involves 4 disulfide linkages per molecule. Thus,

$$n_{\mathrm{Dsb}} \triangleq 4 \cdot n_{\mathrm{Lys}} \approx 1.4 \cdot 10^{-7}\,\mathrm{mol}.$$

In principle, the solvent accessibility of HEWL is restricted to the void volume of Sephadex G-25. V_0 was approximated to about 10 mL in the preliminary default procedure. Neglecting the migration of the mobile phase as well as the portion of glutathione-free denaturation buffer in the gradient a, a C10/40 column completely equilibrated with buffer solution R^+ contains almost 6 µmol of GSSG:

$$n_{\mathrm{GSSG}} \approx c_{\mathrm{GSSG}} \cdot V_0 = 0.0006\ \mathrm{mol/L} \cdot 0.01\,\mathrm{L} = 6 \cdot 10^{-6}\,\mathrm{mol}$$

This would be equivalent to a more than 40-fold excess of GSSG relative to the total count of disulfide bridges per sample. On the one hand, this estimation may be

considered fairly high, as the neglected denaturant gradient makes up the largest volumetric share through which the protein migrates. On the other hand, the diffusion-regulated reconstitution of consumed GSSG from the porous volume reservoir was discounted, too.

Finally, this calculation example was meant to illustrate the preliminary appraisal that the default mode procedure of the urea-gradient SEC basically held considerable potential for economization in terms of glutathione consumption.

The effectiveness of the oxido-shuffling system is suggested to be mainly governed by the ratio of GSH to GSSG, rather than by absolute quantities (BULAJ, 2005). Hence, the investigated approach focused on reducing the portion of glutathione-containing refolding buffer, R^+, without any modification in concentrations. Moreover, the buffer sample was introduced at different sites during gradient formation as described in the corresponding section 3.2.3.2. This was intended to provide additional information on the time-related (kinetically controlled) demand in disulfide shuffling compounds in HEWL refolding.

The comparison of runs G2.1 to G2.3, as depicted in figure 4-10, exemplifies basic similarities as well as deviances of resulting chromatograms after introduction of 2 mL of buffer R^+ at different gradient positions.

It became evident from the detected UV peak near the approximated void volume (~10 mL) in combination with the activity recoveries (see table 4-4) summed up from corresponding fractions that all runs enabled refolding of HEWL in principle.

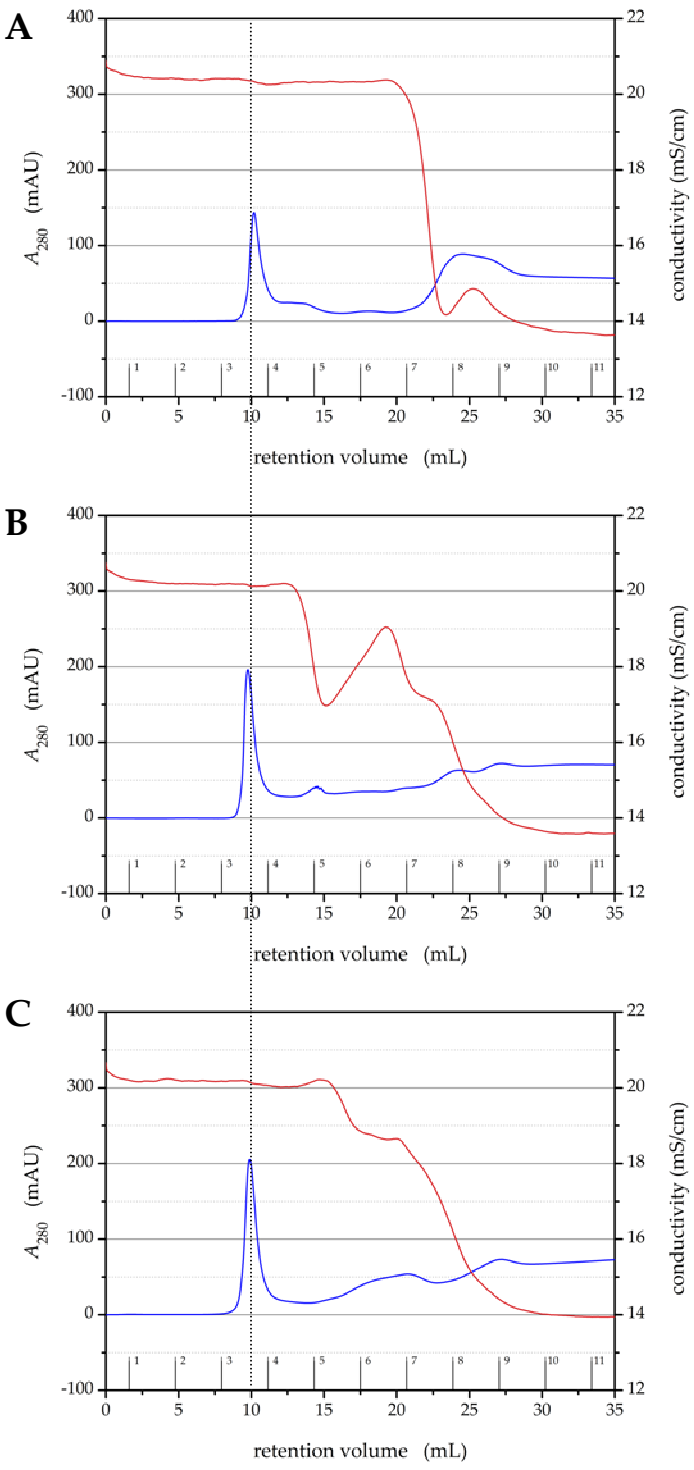

Fig. 4-10: Overview on chromatograms of all experiments involving the injection of 2 mL glutathione-enriched buffer R^+. (**A**) represents FRONT-gradient injection (G2.1), while (**B**) and (**C**) exemplify spiking in the MID (G2.2) and END (G2.3) region, respectively. The dashed line vertically crossing all chromatograms marks the approximate HEWL retention volume in the default setup (~10.0 mL). UV signal is indicated by blue lines, while red traces the conductivity course. Considerable changes in the urea-gradient shape and expansion were observed.

Reproducibly, a pronounced tailing occurred adjacent to this peak of refolded protein. By means of control experiments, this phenomenon was shown to be connected with the additional injection of glutathione-enriched buffer (see appendix 7.C). Thus, the alleged tailing was de facto caused by the superposition of the protein- and glutathione-related peaks. The latter was expected to be shifted depending on the site of buffer injection, yet, could not be traced exactly due to considerable overlapping with further UV signals. Multiple non-separated peaks of medium UV absorption (10-50 mAU) were observed in the following. Related fractions did not exhibit enzymatic activity.

As pointed out in the previous section, the concentration of urea is the main force determining the electrical resistance of utilized chromatography solvents. Thus, the conductivity of the refolding buffers (R^+ and R^-) was distinctly different from that of the denaturing counterpart (buffer D). Hence, the position of the glutathione sample within the urea gradient was principally represented by a peak in the conductivity signal, which is reflected by the non-linearity of the related courses in the given chromatograms.

Tab. 4-4: Overview on quantitative results obtained from all runs introducing 2 mL of glutathione-containing refolding buffer (G2) into different parts of the urea-gradient. Activity analysis was carried out at least 20 hours after sample collection.

Exp. No.	Injection Site	Retention Volume V_R (mL)	Peak Area (mAU · mL)	Activity Recovery (%)
G2.1	FRONT	10.2	255	**55**
G2.2	MID	9.7	240	**39**
G2.3	END	9.9	260	**67**

Consecutively, a causal link is presented in order to explain the interrelations of various impacts, finally resulting in chromatographic irregularities and diminished activity recoveries:

First of all, the gradient formation was interrupted by the injection of the glutathione-enriched buffer sample. The injection valve was subsequently switched back to load

position and an equivalent part of the gradient slope was enclosed in the sample loop. This originated in non-linearity in the gradient formation as reflected by the erratic shape and slope of the conductivity courses. The urea-gradient SEC principle of a smooth buffer transition was therefore disturbed. Migration of denatured and reduced HEWL through the impaired gradient partition increased the probability of protein misfolding and aggregation, which probably induced prolonged retention through non-specific interactions of unfolded polypeptide chains and the solid phase surface as discussed before. Yet, potential aggregate depositions were promptly resolved by the subsequent wash-out with denaturation buffer and were eluted from the column in varying distance to the peak of successfully refolded HEWL. The increased share of misfolded protein proportionally reduced the overall activity recoveries.

In addition to that, a sidewise displacement of the gradient region to lower retention volumes was observed for mid and end gradient injection of glutathione samples. This was indicated by the premature decrease in conductivity after about 13-15 mL. A comparable artifact was not observed with the front gradient injection. However, the buffer transition region of the latter was altered by increased steepness of the gradient slope.

For all distinct glutathione injection sites, a conductivity peak was observed, reflecting the mixing zone of the different solvents involved. Most probably this also affected the UV signal in the gradient region. However, related peaks were found to be indistinguishable from signals caused, for instance, by potential aggregation and normal buffer transition effects.

As mentioned before, only minor variations were observed in the retention volumes of all distinct experiments (~10 mL). The values were consistent with those obtained in the default mode runs, which was in good accordance to the practically unchanged pre-column dead volume.

On the whole, overall yields (39-67 %) were found to be considerably decreased relative to the default experiment outcome (see table 4-4). On the other hand, the

areas of protein-related peaks were generally increased in all experiments, which is likely to be explained by the pronounced tailing and poor peak resolution affecting the setting of a suitable baseline. Potentially, a higher UV detector sensitivity towards particulate aggregates would be another explanation for obtaining higher peak areas but lower activity recoveries.

However, a clear tendency emerged from these quantitative results providing a certain indicating for further method development approaches:

END (G2.3) > FRONT (G2.1) > MID (G2.2)

This hierarchy was particularly emphasized when mass-specific costs were additionally taken into account. Due to the drastic reduction in glutathione consumption, the overall buffer costs per run of experiments G2.1-G2.3 amounted to only 2.86 € or 57 % of the fixed costs per default mode run (4.98 €). Nevertheless, this circumstance hardly demonstrated a considerable advantage over the default mode procedure (see table 4-5). In fact, the moderate overall recoveries obtained by MID (55 %) and END (67 %) gradient glutathione addition allowed at least for a basic improvement in terms of economics and accounted for overall savings of around 11 % and 27 %, respectively. However, the loss of about one third to one half of the starting material is highly disadvantageous regarding a long-term process operation. Therefore, a decision was made to focus on the most promising approach concerning the END gradient injection site as a target for further refinement.

Subsumed from what was explained above, the length and shape of the buffer transition region were substantially affected by the way of additionally implementing the injection of 2 mL glutathione-enriched buffer. On the whole, the introduction of a step-like gradient level according to the original procedure (see section 3.2.3.2) caused a number of artifacts affecting the continuity in gradient linearity and slope.

Tab. 4-5: Overview on mass-specific costs accruing for lysozyme refolding in the first glutathione optimization runs G2.1-G2.3 in comparison to expenditures in the default mode. Negative percent deviations indicate overall cost savings and *vice versa*.

Exp. No.	Mass-Specific Costs (€/mg)	Deviation (%) from Default Mode
V.1 (default)	11.74	± 0
G2.1	10.41	- 11.3
G2.2	14.68	+ 25.0
G2.3	8.54	- 27.3

In revision of these results, an enhanced method protocol was elaborated in order to evade the issue of gradient discontinuity and to provide an ameliorated basis for proper lysozyme refolding.

The concept of this second strategy focused solely on the introduction of glutathione-enriched buffer into the END gradient region. Furthermore, the respective glutathione sample volume was extended to 5 mL. Finally, the weightiest modification was to hold the valve IV-7 in injection position for the complete method duration from the moment of glutathione injection until the end of the wash-out step. Through implementing an extra sample loop in the pre-column flow path, the dead volume increased by the amount of the respective loop size (5 mL) and retention volumes were enlarged accordingly. However, this way of proceeding enabled maintaining the gradient length and slope to their full extent.

In anticipation of the results presented and discussed in the succeeding paragraphs, this protocol is consecutively referred to as the advanced mode of urea-gradient SEC refolding.

Figure 4-11 provides a comparative overview on chromatographic profiles typically observed in urea-gradient SEC runs for the default setup (A; V.1), a 5 mL END gradient injection of glutathione following the initial procedure (B; G5.1) and an advanced mode 5 mL injection (C; A.1).

Apparently, the clear subdivision into a protein peak and a gradient-related region was maintained in all three approaches. While the standard procedure of glutathione

introduction (B) increased the steepness of the buffer transition slope, the advanced mode (C) allowed for retaining the dimensioning and shape of the default setup gradient (A).

As was to be expected, a shift of little more than 5 mL (contributions from the inherent dead volume of the injection valve IV-7 and connective tubings were considerably small) occurred after changing to the advanced mode procedure. This aspect had an effect on the protein peak retention and gradient elution in equal measure. Contemporaneously, a significant peak broadening was observed, which was most probably owed to enhanced dispersive mixing effects within the subjoined sample loop dead volume.

The injection of glutathione-enriched sample buffer, R^+, took place at the same relative point in time for both standard (B) and advanced (C) mode. Therefore, the injection-related peak occurred at the same retention volume (~7-17 mL) in either case. As its appearance coincided with the HEWL peak elution, the glutathione-related peak was reflected by a corresponding protein peak tailing (B) or fronting (C).

Tab. 4-6: Comparison of quantitative results obtained from default run V.1, glutathione-spiking run G5.1 and advanced mode run A.1. Activity analysis was carried out at least 20 hours after sample collection.

Exp. No.	Injection Site	Retention Volume V_R (mL)	Peak Area (mAU · mL)	Activity Recovery (%)
V.1	-	10.0	225	**85**
G5.1	END	10.1	235	**86**
A.1	END	15.1	280	**90**

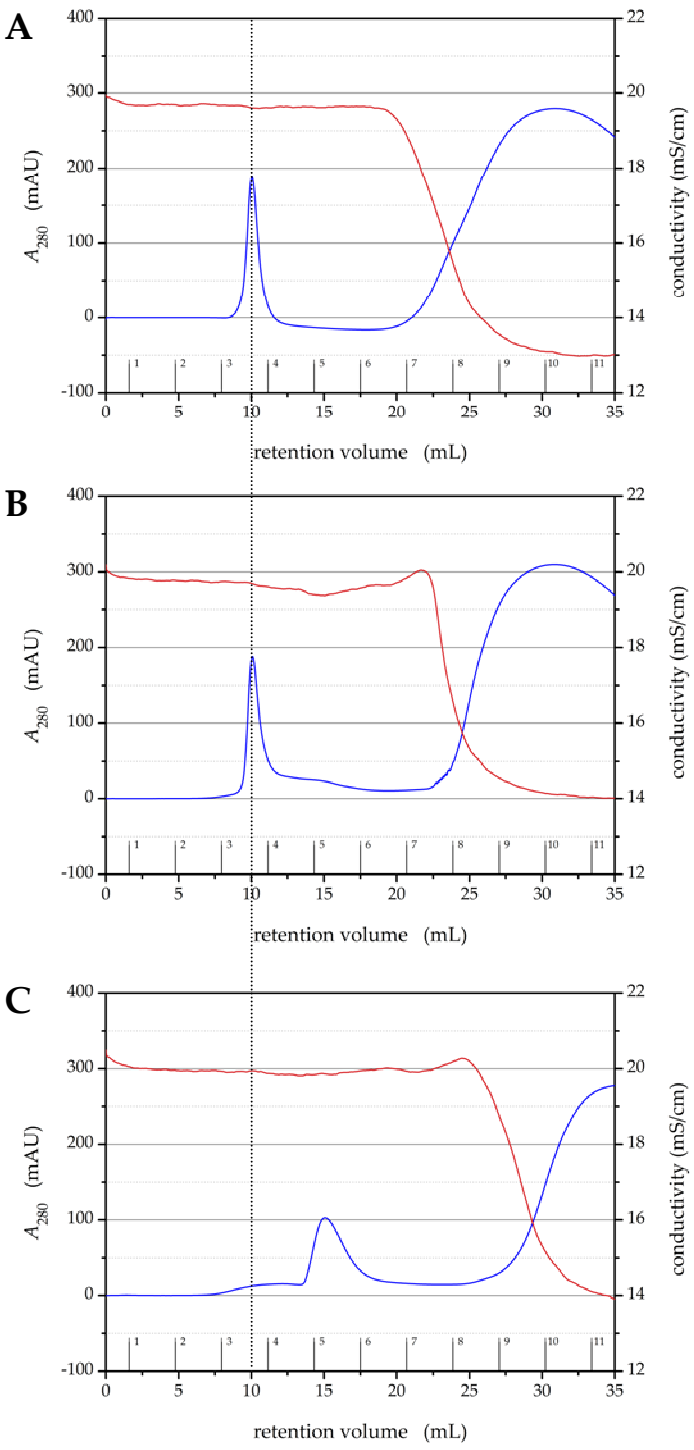

Fig. 4-11: Comparison of the default mode chromatogram (**A**) with results from two runs introducing 5 mL glutathione-enriched buffer in the END gradient position. (**B**) represents the initial procedure, involving a switch of valve IV-7 to load position after glutathione injection. This switch was skipped in the final advanced mode protocol (**C**) and injection position was held until the end of the run. The dashed line vertically crossing all chromatograms marks the approximate HEWL retention volume in the default setup (~10.0 mL). UV signal is indicated by blue lines, while red traces the conductivity course.

Upon application of the revised method protocol, a moderate increase in peak area occurred while enhanced recoveries of refolded lysozyme (90 %) were obtained simultaneously (see table 4-6). In contrast to the results from the initial way of proceeding, the percentage yield of the advanced mode experiment was found to be in the magnitude of recoveries reported for the most successful lysozyme refolding approaches according to literature data (Gu et al., 2001; LI et al., 2004; GENG & WANG, 2007).

The fact that the advanced mode (5 mL of buffer R^+) appeared to be superior even to the default mode (column almost entirely equilibrated with buffer R^+) was unexpected to a certain degree. The phenomenon was assumed not to be predominantly connected to the overall quantity of glutathione available to the protein. Instead, it was suggested that enhanced axial dispersion putatively leads to decreased local protein concentrations thereby shifting the reaction equilibrium in favor of correct folding rather than misfolding and aggregation. In accorcance to this, the basically beneficial influence of dispersive mixing on overall lysozyme refolding yields was recently demonstrated by DING et al. (2011). Subsumed, it may be concluded that most probably the combination of increased axial dispersion with the maintained continuity of the buffer transition region was key to the overall success of the established advanced urea-gradient SEC refolding procedure.

Moreover, a major part of the renaturation process took place after elution from the packed bed, on the one hand. On the other hand, for proteins naturally containing disulfide bonds, the presence of a certain portion of oxido-shuffling reagents is highly recommended to enable efficient refolding to the native-like state. This emphasizes that the actual positioning of the glutathione addition must be carefully attuned in order to ensure that the finally collected sample incorporates the disulfide-shuffling system.

Roughly estimated, a sample of denatured protein will gain access to the glutathione-enriched volumetric partition in the lower third of the column applying the advanced mode strategy. Until this point, the polypeptide chain migrated through

the buffer transition region without any contact to an oxido-shuffling environment. Thus in principle, it may even be questioned whether the GSH/GSSG concentration could be generally adjusted subsequent to the protein elution. For now, this should be comprehended as an outlook on potential future prospects in urea-gradient SEC refolding optimization.

Finally, the economic performance of the advanced mode procedure is to be rated: The corresponding overall buffer costs per run accrued to 2.93 €/mg and in comparison to the default mode, the expenses per run were thereby downsized to about 59 %. Or, in other words, the elaborated advanced protocol provided for total fixed cost savings of around 41 %.

At the same time, the enhanced activity recovery (~90 %) observed for this procedure minimized the total loss of protein and decreased the mass-specific costs to 6.52 € per milligram of refolded HEWL, which is even 44.5 % below the default outcome (see table 4-7).

Tab. 4-7: Overview on mass-specific costs accruing for the refolding of lysozyme by the advanced mode urea-gradient SEC procedure in comparison to expenditures in the default mode. Negative percent deviations indicate overall cost savings.

Exp. No.	Mass-Specific Costs (€/mg)	Deviation (%) from Default Mode
V.1 (default)	11.74	± 0
G5.1	6.52	- 44.5

Through exploring a volumetric partition in which addition of glutathione buffer resulted in high refolding efficiency, the expenditure for oxido-shuffling ingredients (GSH, GSSG) could be decreased dramatically relative to the former default process strategy. This advanced mode of operating the urea-gradient SEC was subsequently applied for renaturation attempts concerning alpha-LA and beta-LG. In general, further lysozyme-specific savings of glutathione consumption are likely to be possible, yet, within the framework of this study a certain margin of GSH/GSSG

availability had to be included with respect to potentially different prerequisites of the other proteins of interest.

4.4 Refolding of Whey Proteins by Advanced Urea-Gradient SEC

As a final objective, the transferability of the elaborated advanced mode was tested by refolding attempts involving another two test proteins, i.e. α-lactalbumin and β-lactoglobulin B. Buffer components and pH values were eventually adopted according to the description in section 3.1.3. Despite of that, sample volumes and protein concentrations were kept constant at 0.2 mL and 2.5 mg/mL, respectively.

4.4.1 Native State Experiments

In preparation of the actual refolding experiments, native state runs were performed in order to elucidate general differences between all three proteins of interest regarding peak characteristics and migration behavior.

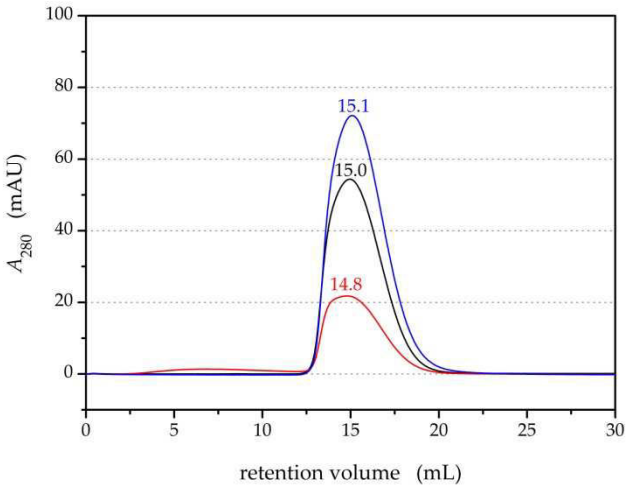

Fig. 4-12: Overlay of native state elution peaks of all test proteins: HEWL (blue), alpha-LA (black) and beta-LG (red). Labels on top of each peak mark the referring retention volumes (mL). The system flow path including the column as well as the precedent 5 mL sample loop were equilibrated with buffer solution R^-. Equal concentrations (2.5 mg/mL) of all proteins were prepared in the same solvent and samples of 0.2 mL were loaded and injected at 0 mL in independent runs.

Tab. 4-8: Major characteristics of native state protein peaks as depicted in figure 4-12.

	Retention Volume V_R (mL)	Peak Area (mAU · mL)
HEWL	15.1	260
alpha-LA	15.0	196
beta-LG	14.8	80

As demonstrated in figure 4-12 and corresponding table 4-8, the most obvious differences observed in the shown chromatograms were the respective peak heights and areas. UV absorption at 280 nm is predominantly governed by tryptophan and tyrosine residues within the primary sequence (just like in fluorescence analysis) and to a minor degree by disulfide bonds and phenylalanine. Therefore, the observed hierarchy reflects roughly the respective content of the aromatic amino acids and intact disulfide bridges of each protein.

Besides these differences in the overall peak appearance, the obtained retention volumes lay close together at (14.95 ± 0.15) mL, whereby the absolute figures decreased with the overall signal intensity of each test protein. A value of around 14.8 mL or less may therefore be taken as a proper approximation of the void volume V_0 for the advanced mode setup.

In particular, the obtained V_R of the native HEWL (15.1 mL) was encountered in good compliance with the retention volume found with refolded lysozyme for the advanced mode system setup as seen in the preceding chapter (see figure 4-11 C). This can be understood as additional evidence for the adequacy of the elaborated advanced urea-gradient SEC on-column refolding method, at least in terms of HEWL renaturation.

The sample volume of 0.2 mL was typically broadened to peak widths of about 7 mL. Putatively, this was for the most part owed to axial dispersion effects, which extensively increased through the additionally implemented extra-column dead volume of the 5 mL sample loop.

4.4.2 Refolding Experiments

In the following paragraphs, results of the advanced mode urea-gradient SEC applied for the refolding of alpha-LA and beta-LG will be presented. Some general remarks shall be made in preparation of the discussed outcome.

Regarding all experiments, chromatographic fractions 5 and 6 appeared to be the only samples showing any protein-specific fluorescence signal in spectrophotometric analysis carried out according to the procedure described in section 3.2.1. Changes in fluorescence intensity and potential shifts in λ_{max} were observed in irregular time intervals over a period of roughly 50-145 hours after sample collection.

All given values of fluorescence intensities used for the calculation of mass recoveries were arithmetic means of emission data obtained within the so called steady state level, rounded to zero decimal places. Exact time spans varied in the course of experiments and will be explicitly declared for each run. The determination procedure was exemplified for the outcome of LA.1 fraction 5 in table 7-2 in appendix 7.D. With respect to the accumulative contributions of random or systematic faults brought up by fluorescence spectrometry, calibration, protein weighing, pipetting, sample fractionation and others, rounding to zero decimal places was assumed to be sufficiently accurate for recovery determinations.

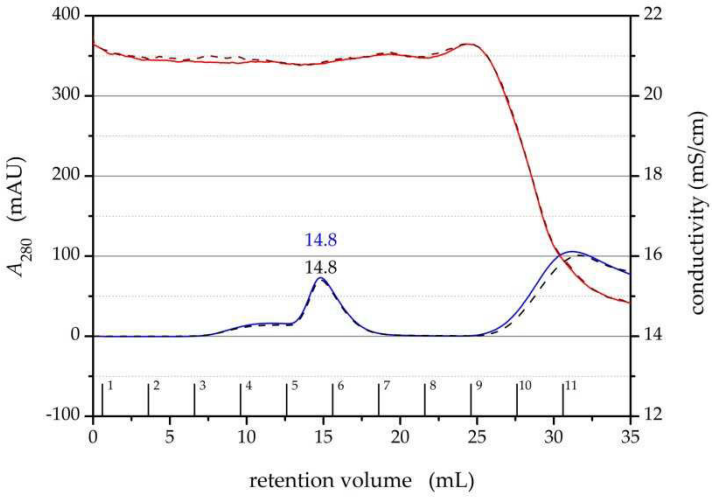

Fig. 4-13: Overlay plot of chromatograms obtained from advanced mode urea-gradient SEC refolding of α-lactalbumin. Data from experiment LA.1 is indicated by the solid blue (A_{280}) and red (conductivity) curves, whereas results of LA.2 are represented by the dashed black (A280) and wine (conductivity) lines. Labels mark the protein elution peak and reflect the respective retention volume.

Tab. 4-9: Characteristics of alpha-LA peaks observed in advanced mode refolding experiments LA.1 and LA.2 in comparison to values obtained from a native state run.

	Retention Volume V_R (mL)	Peak Area (mAU · mL)
alpha-LA (native)	15.0	196
LA.1 (refolded)	14.8	203
LA.2 (refolded)	14.8	195

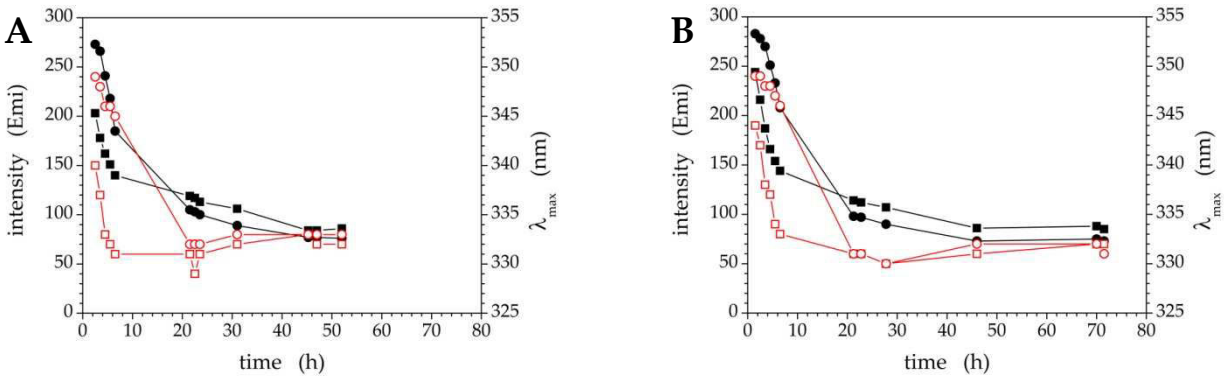

Fig. 4-14: Results from fluorescence analysis of fractions 5 (squares) and 6 (circles) for advanced urea-gradient SEC refolding of α-lactalbumin in experiments LA.1 (**A**) and LA.2 (**B**). Changes in fluorescence intensity are indicated by black lines and filled symbols, while the course of the wavelength at maximum intensity λ_{max} is represented by red lines and empty symbols.

For the first advanced mode urea-gradient SEC refolding experiment using alpha LA (LA.1), the change in fluorescence characteristics was followed between 2.5 and 52 hours (see figure 4-14 A).

A rapid decrease in intensity as well as λ_{max} was observed for both analyzed fractions (5 + 6) within the first 6.5 hours after sample collection. Starting from a wavelength maximum of 340 nm it was supposed that the largest share of alpha-LA eluting in fraction 5 had not reached a native-like conformation within the first hours after elution from the column. Yet, this wavelength was still in significant distance to the λ_{max} obtained for the denatured protein state (353 nm), thereby indicating that the sample molecules possessed a certain degree of three-dimensional structure, which buried intrinsic fluorophores at least in parts. After about 4.5 hours, λ_{max} was shifted to around 332 nm and remained at this level until the end of spectrometric observations at 52 hours. This value is in good accordance to the native state λ_{max} of lactalbumin at 333 nm. It was assumed that alpha-LA underwent further conformational changes and finally persisted in a native-like structure. During the same time span, the fluorescence emission of fraction 5 declined drastically, starting from about 200 and reaching a level of steady intensities after an incubation period of 45 hours (~85). According to the evaluation by means of the linear regression calibration curve, this intensity equaled a mass of about 0.187 mg or a recovery of 37 %.

Fraction 6 showed a distinctly different course, especially in terms of λ_{max}. At the beginning of the fluorescence analysis (2.5 hours) the wavelength of maximum emission was found to be 349 nm. This is very close to the value of 353 nm bound to the denatured and reduced protein state. Therefore, one may conclude that alpha-LA molecules eluting within volumes representing the right-sided peak flank were less adequately folded than molecules eluting earlier. Probably a certain share of the injected denatured sample molecules interacted with the solid phase – either non-specifically or by diffusing partly into close-to-surface pores. This may have caused a slight retention, but those molecules were promptly resolved by the

denaturation buffer used for the wash-out step. Subsequently, retarded proteins would have been able to migrate through the gradient and elute from the column with a short time delay. This delay, in turn, would also affect the kinetic folding state in which the respective share of proteins was examined during the first analytic experiments. However, apart from the divergence over the first hours, λ_{max} of fraction 6 decreased to a similar level as seen in fraction 5 samples and was shown to achieve values around 333 nm after about 21 hours, too. From this observation it was concluded that refolding to a native-like state finally took place in both samples, thus, in all fractions of the alpha-LA peak. The final fluorescence emission intensity observed in fraction 6 was about 77, which corresponds to a mass of 0.167 mg and a recovery 33 %. The overall mass yield of experiment LA.1 thereby added up to a total of 70 %.

The reproduction to this first urea-gradient refolding experiment concerning α-lactalbumin was named LA.2. As can be inferred from the chromatograms (see figure 4-13) and the corresponding peak characteristics (see table 4-9) as well as the fluorescence analysis data (see figure 4-14 B), there was a high degree of equivalence between both runs. A steady state developed after 45 hours likewise. The obtained mass recovery of LA.2 was about 69 %, with fraction 5 accounting for 37 %, while recovery of fraction 6 amounted to 32 %. These values were calculated from steady state emission intensity levels observed in fluorescence analysis of fractions 5 and 6, which were about 85 and 74, respectively.

On the whole, the decline in fluorescence intensity over time was roughly distinguishable into two phases for both fractions of LA.1 and LA.2: Within the first ~10 hours, the intensity decrease was rapid with a great negative slope. In the following, the steepness of this slope appeared to be flattening and a comparably slow emission reduction was observed until reaching the steady state at about 45 hours. Potentially, a link could be made between this two-step decline in fluorescence intensity and the formation of a stable molten globule intermediate state as described by KUWAJIMA (1996) (see section 2.5.2).

In terms of peak areas, the protein-related peaks of LA.1 and LA.2 were highly comparable to the native state (see table 4-9). Measured by this, the overall mass yields of around 70 % appeared to be rather low. The divalent Ca^{2+} ion plays a decisive role in structural reconstitution of α-lactalbumin and was reported to be mandatory for folding and native disulfide formation from the denatured and reduced state (CHRYSINA et al., 2000). Thus, the calcium supply might have been a limiting factor for complete LA refolding. However, no further investigations were made to verify or disprove this assumption.

The advanced mode refolding runs LA.1 and LA.2 were found to be in good concordance. This is true for the fundamental chromatographic profiles as well as the fluorescence analysis data and the consequential mass recoveries. Moreover, the overall process reliability was stressed by the conformity of the proportional contributions from analyzed fractions 5 and 6.

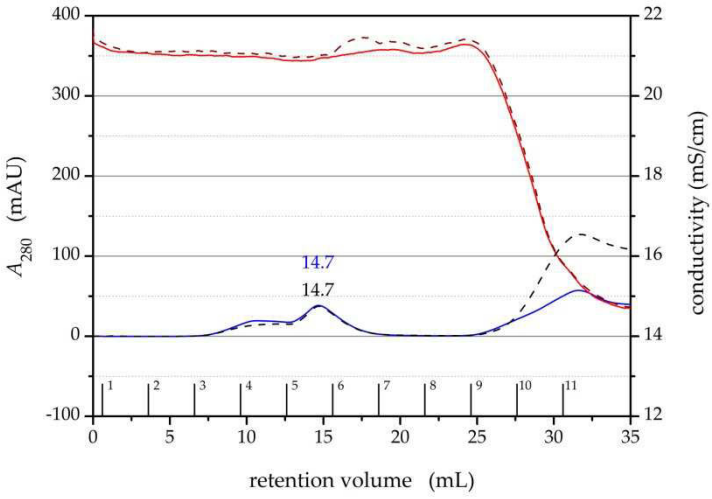

Fig. 4-15: Overlay plot of chromatograms obtained from advanced mode urea gradient SEC refolding of β-lactoglobulin. Data from experiment LG.1 is indicated by the solid blue (A_{280}) and red (conductivity) curves, whereas results of LA.2 are represented by the dashed black (A_{280}) and wine (conductivity) lines.
Labels mark the protein elution peak and reflect the respective retention volume.

Tab. 4-10: Characteristics of beta-LG peaks observed in advanced mode refolding experiments LG.1 and LG.2 in comparison to values obtained from a native state run.

	Retention Volume V_R (mL)	Peak Area (mAU · mL)
beta-LG (native)	14.8	80
LG.1 (refolded)	14.7	125
LG.2 (refolded)	14.7	115

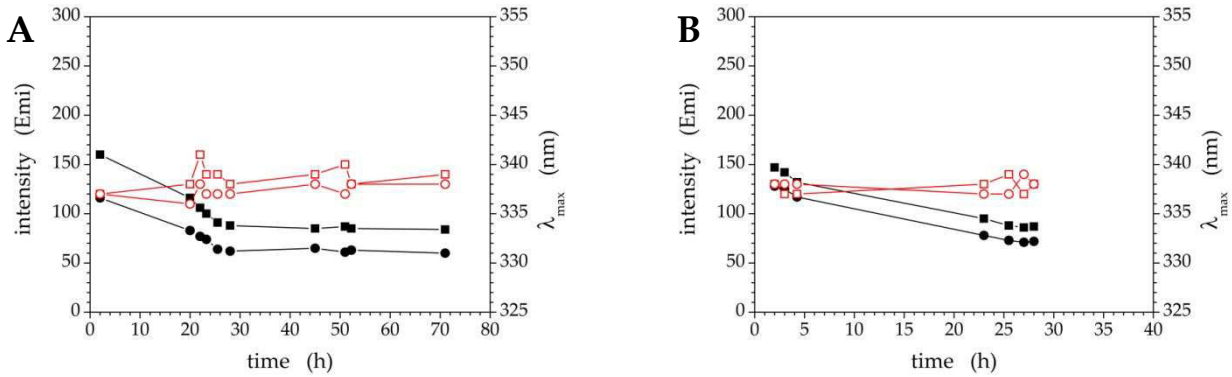

Fig. 4-16: Results from fluorescence analysis of fractions 5 (squares) and 6 (circles) for advanced mode urea gradient SEC refolding of β-lactoglobulin in experiments LG.1 (**A**) and LG.2 (**B**). Changes in fluorescence intensity are indicated by black lines and filled symbols, while the course of the wavelength at maximum intensity λ_{max} is represented by red lines and empty symbols. Time scale differs in (**A**) and (**B**).

In the experiments concerning the advanced mode refolding of β-lacto-globulin B, LG.1 and LG.2, a significant decrease in intensity was measured over time in fractions 5 and 6, just as for alpha-LA analysis (see figure 4-16). Yet, at the same time the maximum wavelength kept almost constant at around (338 ± 1) nm from the beginning of analysis after 2 hours. The observed values were about 1-3 nm higher than the λ_{max} of 336 nm determined for native state beta-LG, thus, possibly pointing at minor differences in the structural conformation. On the whole, the discrepancy in λ_{max} must be put in perspective of its magnitude, which was about one tenth of the equipment parameter of aperture slit width (10 nm), basically implying considerable errors from stray light effects.

A steady state level was reached after approximately 25 hours. For quantification purposes, the arithmetic mean of all emission intensities obtained after this point in time was used for the determination of mass recoveries. β-Lactoglobulin refolding experiments LG.1 and LG.2 accounted for overall yields of 77 % and 82 %, respectively. Out of that, results from fractions 5 were identical (45 %), while recoveries in fraction 6 slightly differed and amounted to 32 % (LG.1) and 37 % (LG.2).

A detailed overview on the quantitative outcome of the advanced mode refolding approaches regarding both whey proteins is provided in table 4-11.

Tab. 4-11: Summary on results obtained in advanced urea-gradient SEC refolding runs regarding whey proteins α-lactalbumin (LA.1, LA.2) and β-lactoglobulin (LG.1, LG.2).

	LA.1		LA.2		LG.1		LG.2	
	frac 5	frac 6	frac 5	frac 6	frac 5	frac 6	frac 5	frac 6
beginning of steady state level (h)	45				25			
fluorescence intensity at steady state (Emi)	85	77	85	74	87	63	87	72
protein concentration (mg/mL)	0.062	0.056	0.062	0.053	0.074	0.054	0.074	0.061
protein mass (mg)	0.187	0.167	0.187	0.160	0.223	0.161	0.223	0.184
mass recovery (%)	37	33	37	32	45	32	45	37
total mass recovery (%)	**70**		**69**		**77**		**82**	

Following a first assumption, a connection could be made between the dimerization behavior of β-lactoglobulin B and the initially occurring decrease in fluorescence emission. According to RENARD et al. (1998) Trp61 is positioned in close proximity to the dimerization interface. Thus, one may assume that fluorescence quenching occurs upon monomer-monomer association.

The steady state phase was identified by the simultaneous appearance of almost constant fluorescence intensities and λ_{max} values. On the one hand, this may be taken as evidence for the hypothesis of dimer reassembling, which might have emerged equilibrium at this state. On the other hand, a similar time-dependent behavior occurred in fluorescence analysis of refolded alpha-LA, which is not prone to significant dimerization facing the given buffer, pH and temperature conditions.

In line with this, the general progression in folding and oxidative disulfide formation within the monomeric form of beta-LG was believed to be primarily responsible for the loss of fluorescence intensity.

Going into some more details, the hardly varying λ_{max} speaks on behalf of the assumption that the major folding process of beta-LG had already been completed at the beginning of analytic examination. Consequently, the initially observed absolute intensity values were considerably lower (~150) relative to those of alpha-LA (~250). Additionally presuming that most cysteine residues of beta-LG were initially found unlinked, the decline in emission intensities during the course of analysis might predominantly be owed to the comparatively slow formation of disulfide bonds. Finally, completion of folding and equilibrium in disulfide reshuffling were achieved for both whey proteins, resulting in approximately equal intensities in the steady state phase. The latter was additionally in good accordance with the phenomenon of similar fluorescence emissions in the native states of alpha-LA and beta-LG (see section 4.1.1).

In comparison of both whey proteins, a loose link may be conjectured between the duration until steady state is reached and the number of disulfide linkages per molecule. While complete folding of beta-LG (2 x Dsb) appeared to be finished after

about 25 hours, the refolding of alpha-LA (4 x Dsb) took almost twice as long with approximately 45 hours. As there was no examination particularly controlling disulfide formation, one has to keep in mind that this interrelationship remains highly speculative. Refolding of lysozyme to the state of maximum activity needed only about 20 hours, although its count and position of disulfide bonds is identical with alpha-LA. This may be considered as another indication that there is no single predominant force governing the respective time delay until equilibrium is reached. Nevertheless, Cys-Cys bridging is likely to play a decisive role.

In principle, the observed emission decrease over time may also be correlated with increased quenching effects from ongoing oxidation of GSH to GSSG, which would also reach steady state after a certain period of time. However, the residual concentration of GSH in fractions 5 and 6 from advanced mode urea-gradient SEC is considerably low. Thus, the occurred drastic reduction of emission intensities solely due to this effect seems implausible.

Focusing on the economic point of view, the level of mass-specific costs varied around approximately 10 € per milligram for refolded whey proteins for the given procedure (see table 4-12). This slightly exceeded the value found for the advanced mode refolding of lysozyme (6.70 €/mg), but still remained in the same order of magnitude. However, these data need not be interpreted as absolute values but should rather be taken as indications to assess the economic feasibility of the overall process, taking into account the expenditure on starting materials.

Tab. 4-12: Mass-specific costs determined for all advanced mode refolding runs concerning alpha-LA and beta-LG.

	LA.1	LA.2	LG.1	LG.2
mass-specific costs (€/mg)	9,68 *)	9,88 *)	10,55	9,96

*) The contribution of $CaCl_2$ costs per run (0.001 €) to total buffer costs (2.927 €) was neglected.

Furthermore, the comparison of the retention volumes as well as protein peak characteristics of results from native state runs (see section 4.4.1) with chromatographic data obtained from the advanced mode refolding experiments showed high congruence regardless of the respective test protein. In principle, the retention volume V_R was slightly lower for the refolded proteins than for their respective native states. It may potentially be stated that this was caused by differing interactions with the solid phase or porous system due to distinctions in hydrodynamic radius or side chain exposures, for instance. Yet, as the divergence between both retention volumes was typically as small as 0.1 mL or 0.3 % of the total column volume, this deviation might as well be owed to statistic variances.

Notwithstanding, the fact that the SEC peaks of native and refolded proteins showed very high congruency, generally gave rise to the expectation of higher final mass yields (of perhaps 90 % or more) in the run-up of data evaluation. A systematic fault adversely affecting the results from fluorescence analysis was considered one probable source of impingement. Especially the inverse dependency of emission intensities and temperatures may have caused an offset in intensity results. Determining the fluorescence emission signal of a reference sample of known concentration might have enabled the adjustment of the respective calibration curve. Yet, due to limited protein resources, this corrective countermeasure was only exemplarily performed once for the run LA.1. The reference was prepared approximately 2 hours prior to measurement. Results are given in figure 4-17. From the corrected calibration curve, an overall mass yield of 84 % (instead of 70 %) could be calculated. This elevated recovery is in better accordance with the expectations deduced from chromatogram conformity of native and refolded samples. Therefore, this way of proceeding may be considered as basically suitable. Nevertheless, it must be pointed out that for a generalization of this observation one could call for additional reassurance experiments.

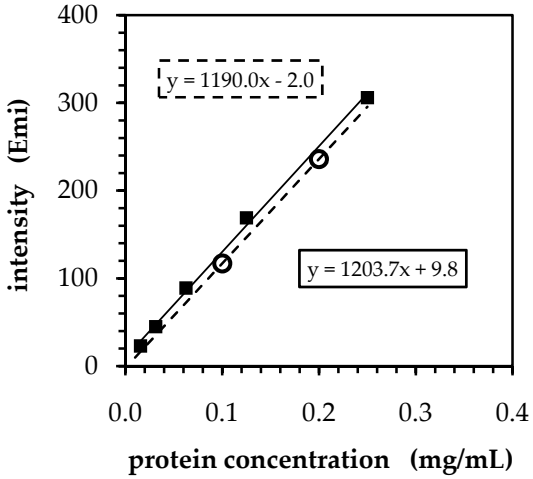

Fig. 4-17: Adjustment of the alpha-LA calibration curve by determining the fluorescence emission from a sample of known concentration. Empty circles mark data coordinates of a 2-point measurement. The slope of a corresponding linear regression curve (dashed line) differed by about 1 % from the original (solid line).

From a general point of view, fluorescence spectrometry was confirmed to be a valuable tool for sample analysis in refolding approaches. Combined provision of structural as well as quantitative information on molecular scale spoke on behalf of its application. Nevertheless, especially its high sensitivity to environmental impacts makes fluorescence analysis basically susceptible to disturbance. Generating protocols for reliable measurements is frequently observed to be complex and time-consuming.

With respect to equipment accessibility, for instance, difference UV absorption and circular dichroism (CD) spectrometry are frequently used as alternatives in renaturation sample analysis. Nevertheless, these methods primarily provide qualitative information on folding states rather than quantification opportunities.

One rather expensive alternative would be the use of ELISA (enzyme-linked immunosorbent assay) kits which are available for both whey proteins. Some of those assays might even claim to specifically detect the native or at least native-like structure conformation of a renatured sample. Nevertheless, experimental data from ELISAs frequently suffer from containing considerable errors and are not trivial to evaluate, e.g. due to cross-reactivity or solvent dependency. Thus, quantification may easily become more elaborate, potentially without even providing favorable qualitative results relative to fluorescence analysis.

Subsumed from the results presented in this chapter, it may be stated that the procedure of refolding by means of the advanced mode urea-gradient SEC was found to be transferable to target proteins other than lysozyme, in principle. The method was simply adapted for the application with two major whey proteins, β-lactoglobulin B and α-lactalbumin. The profiles observed in the chromatograms of alpha-LA and beta-LG refolding were found to be in good accordance to the characteristics identified in corresponding advanced mode HEWL refolding runs. Moreover, the depicted reproductions of all whey protein experiments demonstrated the fundamental reliability in the application of the elaborated procedure. Both test proteins yielded comparably high mass recoveries relative to quantities of 15-25 % frequently found for less sophisticated refolding approaches (SINGH & PANDA, 2005). Nevertheless, by means of intensified and mainly protein-specific optimization efforts, further improvement is to be expected. Possible refinement approaches may include, but are not restricted to the optimization of additive concentrations (e.g. Ca^{2+} molarity in alpha-LA refolding), post-experimental incubation (e.g. temperature control and stirring of collected fractions; adjustment of glutathione content) and – especially in terms of economics prospects – protein loading (e.g. sample volume, concentration) or the establishment of a cyclic process layout.

5. Conclusion

In the course of this work, the principle of size-exclusion-based refolding by means of protein migration through a gradually changing urea environment was demonstrated to be a highly potent and efficient approach in general. Throughout a first experimental series, activity recoveries of around 85 % were achieved upon application of a standard urea-gradient SEC procedure for lysozyme renaturation.

Subsequently, the impact of alterations in gradient length and urea concentrations was investigated in a Design of Experiments (DoE) approach. Related chromatographic profiles were basically as expected. Quantitative results, however, did not allow unambiguous interpretation. Yet, experimental results revealed that the chosen DoE approach did not yield an increase of refolding efficiency. Instead, they indicated a more general incapability of experimental planning to handle the multidimensional task of protein refolding with a common DoE approach.

A fundamental method improvement was achieved by drastically reducing the consumption of the oxido-shuffling compound glutathione. Its usage was restricted to a small volume partition of glutathione-enriched buffer, selectively introduced during column equilibration. This advanced mode of urea-gradient SEC improved the process economy, accounting for fixed cost savings of more than 40 % relative to the original procedure. Notwithstanding the reduced glutathione availability, the recovery of bioactive lysozyme tends to be slightly enhanced.

Finally, this advanced method was adapted for the refolding of the two major whey proteins α-lactalbumin and β-lactoglobulin B. By means of minor procedural modifications, mass recoveries of 70 % and 80 % were obtained for refolding of, respectively.

Long-term analysis by fluorescence spectrometry and enzyme activity assay revealed that all test proteins were found to undergo substantial conformational changes until reaching a steady state within a period of several hours to one or two days after elution from the packed bed. Hence, it has to be concluded that a noticeable part of the folding process takes place in the post-run of gradient SEC experiments.

5. Zusammenfassung

Das Potential der Harnstoff-Gradienten SEC in Bezug auf die Anwendung zur Proteinrenaturierung konnte in der vorliegenden Arbeit grundlegend hervorgehoben werden. Auf Basis der üblichen Vorgehensweise wurden in einer ersten Versuchsreihe Aktivitätsausbeuten von circa 85 % für die Rückfaltung von Lysozym erzielt.

Im Rahmen einer statistischen Versuchsplanung (DoE – Design of Experiments) wurden anschließend die Auswirkungen gezielter Veränderungen an der Länge und den Harnstoffkonzentrationen des Gradientenbereichs untersucht. Die resultierenden Chromatogramme zeigten dabei erwartete Verläufe, jedoch ließen nicht nachvollziehbare Fluktuationen der quantitativen Analysenergebnisse keine eindeutige Interpretation zu. Die experimentellen Ergebnisse zeigten allerdings, dass der gewählte DoE-Ansatz keine Verbesserung der Ausbeute bei der Rückfaltung ermöglichte. Stattdessen wurde deutlich, dass die komplexen Renaturierungsprozesse generell schwer durch eine experimentelle Planung abgebildet werden können, wie sie bei üblichen DoE-Versuchen notwendig sind.

Veränderungen an der Prozessperipherie erlaubten die gezielte Zuführung reduzierter Volumina glutathionhaltigen Puffers während des Equilibrierungsvorgangs. Bei tendenziell sogar leicht erhöhter Ausbeute an bioaktivem Lysozym konnten Einsparungen von mehr als 40 % der Gesamtkosten gegenüber dem konventionellen Verfahren realisiert werden.

Ein letztes Ziel der Arbeit lag in der Anwendung des weiterentwickelten Verfahrens auf die Rückfaltung der beiden Hauptproteine der Molke α-Lactalbumin und β-Lactoglobulin B. Durch geringfügige adaptive Maßnahmen konnten dabei Massenausbeuten von circa 70 % bzw. 80 % erzielt werden.

In Langzeitmessungen mittels Fluoreszenzspektrometrie und Lysozym-Aktivitätsassay wurden für alle Modellproteine konformative Veränderungen nachgewiesen. Erst nach Inkubation der Proben über einen Zeitraum von mehreren Stunden bis zu wenigen Tagen im Anschluss an die Elution wurde ein End- bzw. Gleichgewichtszustand erreicht. Diese Ergebnisse zeigen, dass sich ein nicht unerheblicher Teil des Rückfaltungsprozesses erst nach Abschluss der eigentlichen Harnstoff-Gradienten SEC vollzieht.

6. References

Anfinsen CB (1973) Principles that govern the folding of protein chains. Science 181, 223-230

Anfinsen CB & Scheraga HA (1975) Experimental and theoretical aspects of protein folding. Adv. Prot. Chem. 29, 205-300

Arai M, Ikura T, Semisotnov GV, Kihara H, Amemiya Y & Kuwajima K (1998) Kinetic Refolding of β-Lactoglobulin. Studies by Synchrotron X-ray Scattering, and Circular Dichroism, Absorption and Fluorescence Spectroscopy. J. Mol. Biol. 275, 149-162

Arakawa T & Tsumoto K (2003) The effects of arginine on refolding of aggregated proteins: Not facilitate refolding, but suppress aggregation. Biochem. Biophys. Res. Commun. 304, 148-152

Bulaj G (2005) Formation of disulfide bonds in proteins and peptides. Biotech. Adv. 23, 87-92

Burova TV, Choiset Y Tran V & Haertle T (1998) Role of free Cys121 in stabilization of bovine β-lactoglobulin B. Prot. Eng. 11 (11), 1065-1073

Cabrita LD & Bottomley SP (2004) Protein expression and refolding – a practical guide to getting the most out of inclusion bodies. Biotechnol. Ann. Rev. 10, 31-50

Chan HS & Dill KA (1998) Protein folding in the landscape perspective: Chevron plots and non-Arrhenius kinetics. Proteins 30, 2-33

Chen Y & Leong SSJ (2010) High productivity refolding of an inclusion body protein using pulsed-fed size exclusion chromatography. Process Biochem. 45, 1570-1576

Choi JH, Keum KC & Lee SY (2006) Production of recombinant proteins by high cell density culture of *Escherichia coli*. Chem. Eng. Sci. 61, 876-885

Chrysina ED, Brew K & Acharya KR (2000) Crystal Structures of Apo- and Holo-bovine a-Lactalbumin at 2.2-Å Resolution Reveal an Effect of Calcium on Inter-lobe Interactions. J. Biol. Chem. 47 (274), 37021-37029

De Bernardez Clark E (1998) Refolding of recombinant proteins. Curr. Opin. Biotechnol. 9, 157-163

De Bernardez Clark E (2001) Protein refolding for industrial processes. Curr. Opin. Biotechnol. 2 (12), 202-207

Ding Y, He L & Middelberg APJ (2008) Dispersion-enhanced chromatography refolding of denatured protein. Chem. Eng. Sci. 63, 4333-4341

Ding Y, Chuan YP, He L & Middelberg APJ (2011) Dispersive mixing and intraparticle partitioning of protein in size-exclusion chromatographic refolding. J. Chromatogr. A 1218, 8503-8510

Divsalar A, Saboury AA, Moosavi-Movahedi AA, Mansoori-Torshizi H (2006) Comparative analysis of refolding of chemically denatured β-lactoglobulin types A and B using the dilution additive mode. Int. J. Biol. Macromol. 38, 9-17

Dobson CM (2004) Principles of protein folding, misfolding and aggregation. Semin. Cell Dev. Biol. 15, 3-16

Dong XY, Wang Y, Shi JH & Sun Y (2002) Size exclusion chromatography with an artificial chaperone system enhanced lysozyme renaturation. Enz. Microb. Tech. 30, 792-797

Eigel WN, Butler JE, Ernstrom CA, Farell HM, Harwalker VR, Jenness R & Whitney RML (1984) Nomenclature of proteins of cow's milk: fifth revision. J. Dairy Sci. 67, 1599-1631.

Formoso C & Forster LS (1975) Tryptophan Fluorescence Lifetimes in Lysozyme. J. Biol. Chem. 10 (250), 3738-3745

Formoso C & Forster LS (1976) Tryptophan fluorescence and homology in lysozymes and α-lactalbumins. Biochem. Biophys. Act. 427, 377-386

Freydell EJ, van der Wielen LAM, Eppink MHM & Ottens M (2010) Size-exclusion chromatographic protein refolding: Fundamentals, modeling and operation. J. Chromatogr. A 1217, 7723-7737

Galani D & Owusu-Apenten RK (1999) Beta-lactoglobulin denaturation by dissociation-coupled unfolding. Food Res. Int. 32, 93-100

Gao Y., Guan Y., Yao S. & Cho M. (2003) Lysozyme refolding at high concentration by dilution and size-exclusion chromatography. J. Zhejiang Univ. Sci. 2 (4), 136-141

Geng X & Wang C (2007) Protein folding liquid chromatography and its recent developments. J. Chromatogr. B 849, 69-80

Gottschalk M, Nilsson H, Roos H & Halle B (2003) Protein self-association in solution: The bovine β-lactoglobulin dimer and octamer. Prot. Sci. 12, 2404-2411

Gu Z, Su Z & Janson JC (2001) Urea gradient size-exclusion chromatography enhanced the yield of lysozyme refolding. J. Chromatogr. A 918, 311-318

Gu Z, Weidenhaupt M, Ivanva N, Pavlov M, Xu B, Su ZG & Janson JC (2002) Chromatographic Methods for the Isolation of, and Refolding of Proteins from *Escherichia coli* Inclusion Bodies. Prot. Expr. Purif. 25, 174-179

Hamada D & Dobson CM (2002) A kinetic study of β-lactoglobulin amyloid fibril formation promoted by urea. Prot. Sci. 11, 2417-2426

Himmel ME, Baker JO & Mitchell DJ (1995) taken from: Handbook of size exclusion chromatography (Wu CS, Ed.) 2nd Series: Chromatographic science, Vol. 69, Marcel Dekker Inc., New York; 409-428

Imoto T, Forster LS, Rupley JA & Tanaka F (1972) Fluorescence of Lysozyme: Emissions from Tryptophan Residues 62 and 108 and Energy Migration. Proc. Nat. Acad. Sci. USA 5 (69), 1151-1155

Irwin DM, Biegel JM & Stewart CB (2011) Evolution of the mammalian lysozyme gene family. BMC Evol. Biol. 11 (166)

Janson JC (2011) Protein Purification: Principles, High Resolution Methods, and Applications. Vol. 54, 3rd edition, John Wiley & Sons, Hoboken, pp. 51-91

Jungbauer A & Kaar W (2007) Current status in technical protein refolding. J. Biotechnol. 128, 587-596

Kawahara K & Tanford C (1966) Viscosity and Density of Aqueous Solutions of Urea and Guanidine Hydrochloride. J. Biol. Chem. 13 (241), 3228-3232

Kontopidis G, Holt C & Sawyer L (2004) Invited Review: β-Lactoglobulin: Binding Properties, Structure, and Function. J. Dairy Sci. 87, 785-196

Kopito RR (2000) Aggreosomes, inclusion bodies and protein aggregation. Trends Cell Biol. 10, 524-530

Kronman MJ, Sinha SK & Brew K (1981) Characteristics of the Binding of Ca^{2+} and Other Divalent MetIaoln s to Bovine α-Lactalbumin. J. Biol. Chem. 256 (16), 8582-8587

Lakowicz JR (1999) Principles of Fluorescence Spectroscopy. 2nd edition, Kluwer Academic / Plenum Publishers, New York

Lilie H, Schwarz E & Rudolph R (1998) Advances in refolding of proteins produced in *E. coli*. Curr. Opin. Biotechnol. 9, 497-501

Li M, Zhang G & Su Z (2002) Dual gradient ion-exchange chromatography improved refolding yield of lysozyme. J. Chromatogr. A 959, 113-120

Li M, **Su Z & Janson JC** (2004) In vitro refolding by chromatographic procedures. Prot. Expr. Purif. 33, 1-10

Maenaka K, Matsushima M, Song H, Sunada F, Watanabe K & Kumagai I (1995) Dissection of protein-carbohydrate interactions in mutant hen egg-white lysozyme complexes and their hydrolytic activity. J. Mol. Biol. 247, 281-293

Malavasi NV, Foguel D, Bonafe CFS, Braga CACA, Chura-Chambi RM, Vieira JM & Morganti L (2011) Protein refolding at high pressure: Optimization using eGFP as a model. Process Biochemistry 46, 512-518

Masuda T, Ueno Y & Kitabatake N (2001) Sweetness and Enzymatic Activity of Lysozyme. J. Agric. Food Chem. 49 (10), 4937-4941

McKenzie HA & White FH (1991) Lysozyme and α-Lactalbumin: Structure, Function, and Interrelationships. Adv. Prot. Chem. 41, 173-315

Middelberg APJ (2002) Preparative protein refolding. Trends Biotechnol. 10 (20), 437-443

Misawa S & Kumagai I (1999) Refolding of therapeutic proteins produced in *Escherichia coli* as inclusion bodies. Biopoly. 51, 297-307

Mulvihill DM & Donovan M (1987) Whey Proteins and their Thermal Denaturation – A Review. Ir. J. Food Sci. Technol. 11, 43–75

Murphy RM & Tsai AM (2006) Misbehaving Proteins: Protein (Mis)Folding, Aggregation, and Stability. Springer Science+Business Media, New York, pp. 3-16

Naqvi Z, Khan RH & Saleemuddin M (2010) A procedure for the purification of beta-lactoglobulin from bovine milk using gel filtration chromatography at low pH. Prep. Biochem. Biotechnol. 40 (4), 326-336

Oliveira KMG, Valente-Mesquita VL, Botelho MM, Sawyer L, Ferreira ST & Polikarpov I (2001) Crystal structures of bovine β-lactoglobulin in the orthorhombic space group $C222_1$: Structural differences between genetic variants A and B and the features of the Tanford transition. Eur. J. Biochem. 268, 477-483

Pace NC (1990) Measuring and increasing protein stability. Trends Biotechnol. 8, 93-98

Pike AC, Brew K & Acharya KR (1996) Crystal structures of guinea-pig, goat and bovine alpha-lactalbumin highlight the enhanced conformational flexibility of regions that are significant for its action in lactose synthase. Structure 4 (6), 691-703

Qoronfleh MW, Hesterberg LK & Seefeldt MB (2007) Confronting high-throughput protein refolding using high pressure and solution screens. Protein Expr. Purif. 2 (55), 209-224

Renard D, Lefebvre J, Griffin MCA & Griffin WG (1998) Effects of pH and salt environment on the association of β-lactoglobulin revealed by intrinsic fluorescence studies. Int. J. Biol. Macromol. 22 (1), 41-49

Rinas U & Bailey JE (1992) Protein compositional analysis of inclusion bodies produced in recombinant *Escherichia coli*. Appl. Microbiol. Biotechnol. 37, 609-614.

Rouessac F, **Rouessac A** (2007) Chemical Analysis: Modern Instrumentation Methods and Techniques. 2nd edition, John Wiley & Sons Ltd., Chichester, pp. 241-259

Sakurai K & Goto Y (2002) Manipulating Monomer-Dimer Equilibrium of Bovine β-Lactoglobulin by Amino Acid Substitution. J. Biol. Chem. 277, 25735-25740

Samuel D, Kumar TKS, Ganesh G, Jayaraman G, Yang PW, Chang MM, Trivedi VD, Wang SL, Hwang KC, Chang DK & Yu C (2000) Proline inhibits aggregation during protein refolding. Prot. Sci. 9, 344-352

Sanyal G, Kim E, Thompson FM & Brady EK (1989) Static quenching of tryptophan fluorescence by oxidized dithiothreitol. Biochem. Biophys. Res. Commun. 2 (165), 772-781

Shiloach J & Fass R (2005) Growing *E. coli* to high cell density – A historical perspective on method development. Biotechnol. Adv. 23, 345-357

Shugar D (1952) The measurement of lysozyme activity and the ultra-violet inactivation of lysozyme. Biochim. Biophs. Act. 8, 302-309

Siebertz K, van Bebber D & Hochkirchen T (2010) Statistische Versuchsplanung: Design of Experiments (DoE). Springer-Verlag, Berlin, Heidelberg

Singh SM & Panda AK (2005) Solubilization and Refolding of Bacterial Inclusion Body Proteins. J. Biosc. Bioeng. 4 (99), 303-310

Speed MA, Wang DI & King J (1996) Specific aggregation of partially folded polypeptide chains: the molecular basis of inclusion body composition. Nat. Biotechnol. 14, 1283-1287

Sriumolbas N, Panbangred W, Sriurairatana S & Meevootisom V (1997) Localization and characterization of inclusion bodies in recombinant *Escherichia coli* cells overproducing penicillin G acylase. Appl. Microbiol. Biotechnol. 4 (47), 373-378

Stevens R, Stevens L & Price NC (1983) The Stabilities of Various Thiol Compounds used in Protein Purifications. Biochem. Educ. 11 (2), 70

Su Z, Lu D & Liu Z (2011) Refolding of inclusion body proteins from *E. coli*. Taken from: Protein Purification: Principles, High Resolution Methods, and Applications. (Janson JC, Editor), vol. 54, 3rd edition, John Wiley & Sons, Hoboken, pp. 319-338

Swietnicki W (2006) Folding aggregated proteins into functionally active forms. Curr. Opin. Biotechnol. 17, 367–372

Timasheff SN & Xie G (2003) Preferential interactions of urea with lysozyme and their linkage to protein denaturation. Biophys. Chem. 105, 421-448

Townend R (1964) β-Lactoglobulins A and B: The Environment of the Asp/Gly Difference Residue. Arch. Biochem. Biophys. 109, 1-6

Tsumoto K, Ejima D, Kumagai I & Arakawa T (2002) Practical considerations in refolding proteins from inclusion bodies. Protein Expr. Purif. 1 (28), 1-8

Vallejo LF, Rinas U (2004) Strategies for the recovery of active proteins through refolding of bacterial inclusion body proteins. Microb. Cell Fact. 3 (11)

Van den Berg B, Chung EW, Robinson CV & Dobson CM (1999) Characterisation of the Dominant Oxidative Folding Intermediate of Hen Lysozyme. J. Mol. Biol. 290, 781-796

Vazquez E, Corchero JL & Villaverde A (2011) Post-production protein stability: trouble beyond the cell factory. Microbial Cell Factories 10:60

Veprintsev DB, Permyakov SE, Permyakov EA, Rogov VV, Cawthern KM & Berliner LJ (1997) Cooperative thermal transitions of bovine and human apo-α-lactalbumins: evidence for a new intermediate state. Fed. Eur. Biochem. Soc. Lett. 412, 625-628

Verheul M, Pedersen JS, Roefs SPFM & de Kruif KG (1999) Association Behavior of Native β-Lactoglobulin. Biopoly. 49 (1), 11-20

Vivian JT & Callis PR (2001) Mechanisms of Tryptophan Fluorescence Shifts in Proteins. Biophys. J. 80, 2093-2109

Wang C & Cheng Y (2010) Urea-Gradient Protein Refolding in Size Exclusion Chromatography. Curr. Pharm. Biotechnol. 11, 289-292

Wang SSS, **Chang CK**, **Peng MJ** & **Liu HS** (2006) Effect of glutathione redox system on lysozyme refolding in size exclusion chromatography. Food Bioprod. Process. 84 (C1), 18-27

Wang GZ, Dong XY & Sun Y (2009) The role of disulfide bond formation in the conformational folding kinetics of denatured/reduced lysozyme. Biochem. Eng. J. 46, 7-11

Wehry EL (1997) Molecular Fluorescence and Phosphorescence Spectrometry. Taken from: Handbook of Instrumental Techniques for Analytical Chemistry. (Settle F, Ed.) Prentice Hall PTR, Upper Saddle River, NJ; pp. 507-539

Wilms D (2010) Renaturierung von Lysozym mittels Harnstoff-Gradienten-SEC. Bachelor's thesis, University of Applied Sciences (HAW) Hamburg

Zumdahl SS & Zumdahl (2008) Chemistry. 8th edition, Brooks/Cole, Belmonte, pp. 497-536

7. Appendices

A Valve Position Setup for the Injection of Two Samples

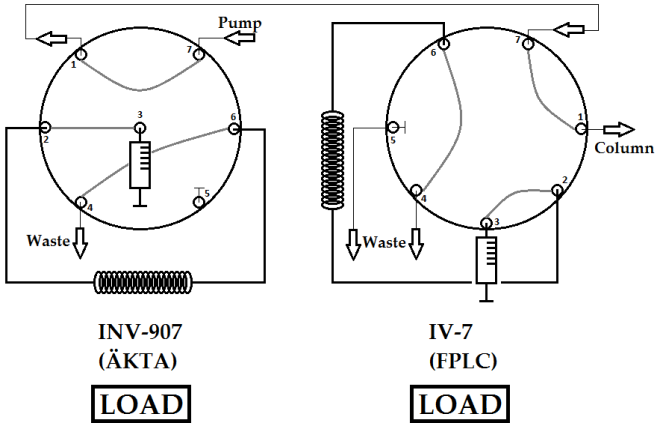

Fig. 7-1: Valve positions of injection valves INV-907 and IV-7 during the column equilibration step. Buffer was driven directly onto the column bypassing both sample loops.

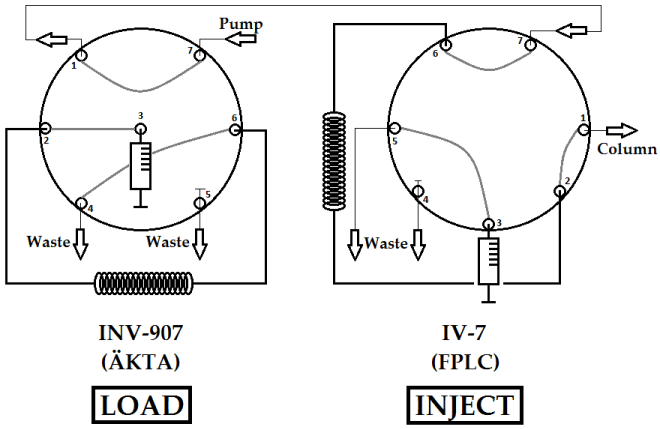

Fig. 7-2: Valve positions during injection of glutathione-enriched refolding buffer. Glutathione buffer prefilled in the sample loop no. 2 of IV-7 was washed onto the column, while the flow path still bypassed the first sample loop in INV-907.

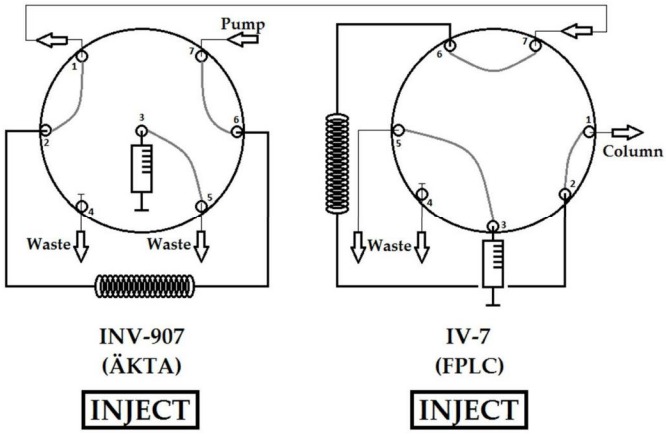

Fig. 7-3: Valve positions during injection of the denatured and reduced protein sample. After the glutathione-containing buffer was transferred to the column and the gradient formation was completed, the protein sample was injected from INV-907 sample loop no. 1.

B Viscosity of Aqueous Urea Solutions

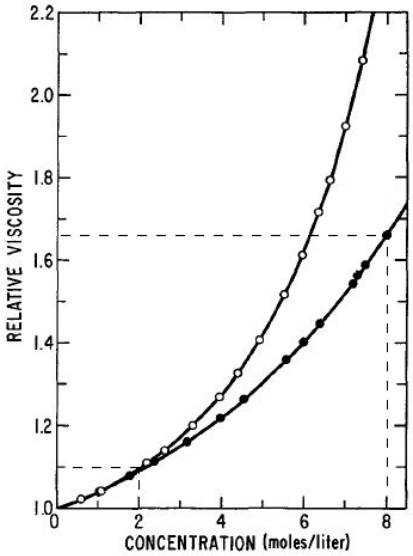

Fig. 7-4: The change in relative viscosities of aqueous solutions of urea is represented by filled circles. Dashed lines mark data points corresponding to urea concentrations found in buffer solutions D (top right) and R (bottom left). Empty circles refer to data of guanidinium hydrochloride and were not discussed in this work.
(modified from KAWAHARA & TANFORD, 1966)

Tab. 7-1: Control experiments demonstrating the diminishing impact of high molar concentrations of urea on the conductivity of aqueous solutions containing sodium chloride. TRIS was additionally tested in experiments no. 2 and 4, and a further slight decrease of conductivity by around 3.5 % was observed. All test solutions were prepared using demineralized water (0 mS/cm). The influence of DTT and GSH/GSSG was not explicitly examined.

Exp. No.	1	2	3	4
Test solution	0.2 M NaCl	0.2 M NaCl + 0.1 M TRIS	0.2 M NaCl + 8 M Urea	0.2 M NaCl + 0.1 M TRIS + 8 M Urea
Conductivity (mS/cm)	20.52	19.85	8.44	8.14

C Peak after Sample Injection of Glutathione-Enriched Refolding Buffer

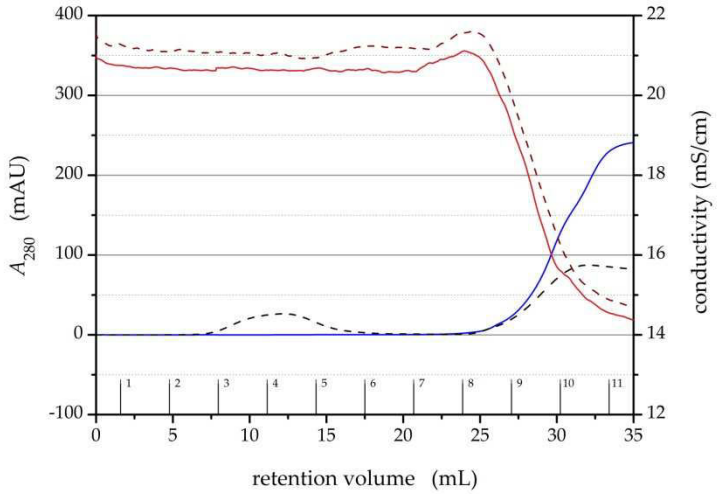

Fig. 7-5: Overlay of two control experiments verifying the cause of the low-absorption UV peak between approximately 7.5 and 17.5 mL. Equilibration and gradient formation was done using solvent D and glutathione-free buffer, R^-. Dashed lines refer to the courses of UV (black) and conductivity (wine) obtained following the advanced mode setup including the injection of 5 mL buffer R^+. Solid lines represent UV signal (blue) and conductivity (red) of an advanced mode run including a blank injection of 5 mL buffer solution R^-. No protein sample was loaded in both experiments and the relevant peak occurred only in case of glutathione injection.

D Approximation of Steady State Fluorescence of Refolded Whey Proteins

Tab. 7-2: Exemplary approximation of steady state fluorescence intensity employed for recovery calculation using data from experiment LA.1 as an example. In this case, steady state was assumed for $t \geq 45$ h. The final value is marked in bold type.

time (h)	fluorescence intensity (Emi)	arithmetic mean (Emi)
45.25	84	84.66 ≈ **85**
47	84	
52	86	